Cooling Strategy for Effective Automotive Power Trains: 3D Thermal Modeling and Multi-Faceted Approach for Integrating Thermoelectric Modules into Proton Exchange Membrane Fuel Cell Stack

by

Dilip Ramani

A Thesis Presented in Partial Fulfillment
of the Requirements for the Degree
Master of Science in Technology

Approved November 2014 by the
Graduate Supervisory Committee:

Abdel Ra'ouf Mayyas, Chair
Keng Hsu
Arunachalanadar Madakannan

ARIZONA STATE UNIVERSITY

December 2014

ABSTRACT

Current hybrid vehicle and/or Fuel Cell Vehicle (FCV) use both FC and an electric system. The sequence of the electric power train with the FC system is intended to achieve both better fuel economies than the conventional vehicles and higher performance. Current hybrids use regenerative braking technology, which converts the vehicles kinetic energy into electric energy instead of wasting it. A hybrid vehicle is much more fuel efficient than conventional Internal Combustion (IC) engine and has less environmental impact.

The new hybrid vehicle technology with it's advanced with configurations (i.e. Mechanical intricacy, advanced driving modes etc) inflict an intrusion with the existing Thermal Management System (TMS) of the conventional vehicles. This leaves for the opportunity for now thermal management issues which needed to be addressed. Till date, there has not been complete literature on thermal management issued of FC vehicles. The primary focus of this dissertation is on providing better cooling strategy for the advanced power trains. One of the cooling strategies discussed here is the thermo-electric modules.

The 3D Thermal modeling of the FC stack utilizes a Finite Differencing heat approach method augmented with empirical boundary conditions is employed to develop 3D thermal model for the integration of thermoelectric modules with Proton Exchange Membrane fuel cell stack. Hardware-in-Loop was designed under pre-defined drive cycle to obtain fuel cell performance parameters along with anode and cathode gas flow-rates and surface temperatures. The FC model, combined experimental and finite differencing nodal net work simulation modeling approach which implemented heat generation across the stack to depict the chemical composition process. The structural

and temporal temperature contours obtained from this model are in compliance with the actual recordings obtained from the infrared detector and thermocouples. The Thermography detectors were set-up through dual band thermography to neutralize the emissivity and to give several dynamic ranges to achieve accurate temperature measurements. The thermocouples network was installed to provide a reference signal.

The model is harmonized with thermo-electric modules with a modeling strategy, which enables optimize better temporal profile across the stack. This study presents the improvement of a 3D thermal model for proton exchange membrane fuel cell stack along with the interfaced thermo-electric module. The model provided a virtual environment using a model-based design approach to assist the design engineers to manipulate the design correction earlier in the process and eliminate the need for costly and time consuming prototypes.

DEDICATION

This dissertation is dedicated to my mother, father and all my family who have supported me all the way through my studies.

Also, this work is dedicated to all my friends in India and the United states who have been a great support for me.

ACKNOWLEDGMENTS

I would like to acknowledge the guidance of my advisor Dr. Abdel Ra'ouf Mayyas for his continuous support throughout this work. I would also like to thank my committee members Dr. A.M. Kannan and Dr. Kheng Hsu for their valuable inputs and support to enhance this work.

I would also like to appreciate the generosity of Thermoanalytics Inc. for their kind for their support with the software needed to work for this dissertation. I would like also to acknowledge Mr. Tony Schwenn, Mr. Steven Patterson and Mr. Joshua Morley for their technical support. My special thanks go to my research teammates Govind, Subham and Hari for their support during experiments and modeling.

TABLE OF CONTENTS

Page

LIST OF TABLES

LIST OF FIGURES

NOMENCLATURE

PEM: Proton/ Polymer Exchange/Electrolyte Membrane

MEA- Membrane Electrode Assembly

FCV: Fuel Cell Vehicle

BEV: Battery Electric Vehicle

FCHEV: Fuel Cell Hybrid Electric Vehicle

EPA: Environmental Protection Agency

FUDS: Federal Urban Driving Schedule

FHDS: Federal Highway Driving Schedule

TEM\TEC- Thermoelectric Module\ Thermoelectric Cooler

FDC- Finite Differencing Code

FEM- Finite Element Method

FLIR- Forward looking infrared

NHR- Net Heat exchange Rate

IR- Infrared

CHAPTER ONE

1. INTRODUCTION

1.1 Proton Exchange Membrane Fuel cell (PEMFC) technology

PEM fuel cells are the most promising of various existing fuel cell systems because of simplicity of its design and low temperature operations. The attractiveness of this fuel cell system has increased significantly within the past five years because of reduced use of the active catalyst materials, improved conductivity, water permeability, and better thermal stability. PEMFC operate on pure hydrogen have several of attributes which makes them an attractive alternative to replace internal combustion(IC) engines. Some of the advantages are high efficiency, faster start up, zero emission and low costs. Another important asset of FCs that they are extensible and could be stacked until the desired power output is reached. As the FCs operates so quietly that they lessen noise and air pollution. Furthermore, the waste heat from a fuel cell could possibly used to provide hot water or space heating for an office or hotel.

In a PEMFC, hydrogen gas flows to the anode. There, with the help of the catalyst, the molecules are broken down into protons (hydrogen ions) and electrons. The positively charged protons go through the porous membrane and migrate toward the cathode as illustrated in Figure.1. On a stack level, this flow can be used to power electric applications. At the cathode, the hydrogen protons, the electrons from the external circuit and oxygen from the air combine to form water. The reaction is exothermic, which means that it generates lot of heat.

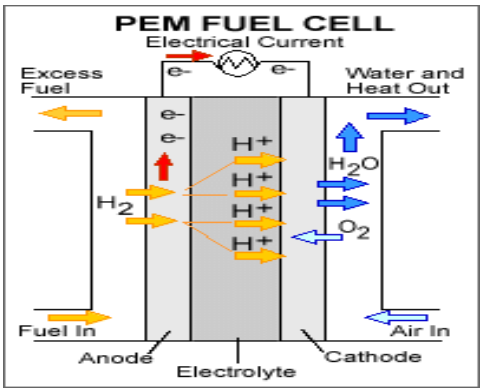

Figure1: PEM working principle

PEMFC operates at a temperature of about 80^0 C in which fusion of hydrogen and Air to produce Electric current and water. Along with this a lot of heat is also produced. This temperature is dictated by the polymer membrane which is Nafion. These membranes exhibit proton conductivity only in the hydrated form. This emphasizes that the waste heat needs to be removed so that the membranes don't dehydrate. The thermal and water management issues are due to the operating temperature < 90 ^oC, with air at the cathode at relatively lower pressure. [1] Thermal management of the heat produced in the cells is a major challenge. This suggests that thermal heat and water produced need to be managed efficiently to maintain the performance and efficiency of the fuel cell system.

1.2 Motivation

Among various fuel cell types, proton exchange membrane fuel cells (PEMFCs) are the most promising for automotive applications due to their higher power density and lower operating temperature. It is expected to play a key role in future automotive technology. Thermal management is vital for both conventional vehicles and the hybrid vehicles, as it defines vehicle's overall performance. Generally, thermal modeling assists in analyzing thermal loads on under-hood components for better thermal packaging in addition to the utilization strategies of Automotive parts. This leads to exhaust emissions reduction

and better thermal efficiency. Furthermore, these improvements will result in weight and cost reduction in addition to devising new control strategies. The hybrid vehicles modules add more complexity to the vehicle Thermal Management System (TMS). However, establishing high-quality TMS for the hybrid vehicle is still a dispute due to fact that the advanced power-trains are still an additive to the architecture of the current vehicles. [2]

The primary objective of this study is to predict the thermal temperature distribution of a PEM fuel cell at varying loads to identify thermal interaction of the cells. This thermal distribution is optimized using a thermo-electric module. As the future world is of FCV's & hybrid vehicles, packaging and thermal prediction of fuel cell plays a major role in the efficient design of any power train.

1.3 Problem Statement

Predicting the thermal behavior of each and every component in a fuel cell system by giving their exact boundary conditions using analysis software and verify the results obtained experimentally with Infrared (IR) Camera. The interaction of heat generated in a fuel cell on other components is also studied. It is our prime concern to know how the thermal management is achieved in FCV's & HEV's. As an advancement, the TMS could be integrated with is devised in today's world so that we can efficiently design in FCVs.

1.4 Approach

An integrated experimental and finite differencing simulation modeling approach is adopted using thermography detectors, to achieve accurate temperature measurements. This was attained through 2D spatial and transient temperature profiles to obtain the boundary conditions of the FC stack. The actual boundary conditions were then set up through finite difference nodal network simulation code for solving refined

thermal/fluid systems with slightest user interaction(RadTherm), to develop 3D Thermal model. The primary analysis focused on Nexa 1.2 KW FC system to study the critical thermal management issue. A comprehensive testing practice was implemented in order to evaluate the thermal performance of the FC stack under different load conditions while overseeing the thermal performance.

The mode we adopted was compiling each and every component of a fuel cell using conventional CAD package (solid works). The next step involved meshing the model using a powerful tool named ANSA was employed. This procedure is critical, to break down the surfaces of the model into finite elements to improve the accuracy of the model for better thermal analysis. Furthermore, the entire FC stack component was imported in to analysis software called Radtherm, the perform thermal analysis could be performed by applying both front & back boundary conditions along with the material properties for each component depending on their function. The next step of the analysis implicates the comparison between the Radtherm results with results obtained from Infra-red (IR) Camera data. As an extension of the procedure, the 3D model was incorporated with thermo-electric modules to optimize the thermal performance of the FC stack. The results of which are discussed in the future sections. Based on the current drawn, flow rates of hydrogen and air, of the anode and cathode are calculated respectively. But the maximum flow rates for hydrogen and air is given based on the Stoich on the anode and cathode respectively.

CHAPTER TWO

2. LITERATURE REVIEW

2.1 Existing Literature

There has been an intensive research conducted in order to improve the performance of the PEM Fuel Cells. The existing or published literature discussed the TMS of the vehicle through thermal modeling automotive vehicle subsystems. However, such approaches required thorough computations combined with sever assumptions to simplify the model and reduce the data content. For instance, Setareh et al. [3] developed a 3D numerical thermal model to analyze the heat transfer and predict the temperature distribution in air-cooled PEMFCs. The Air-cooled FC system served two purposes, the cooling function and cathode flow which reduced the overall cost of auxiliary systems. The prime objective of this paper was to develop a 3D thermal model of an air-cooled PEMFC stack which helps to determine the temperature distribution and heat transfer coefficients. This 3-D model could be used for design of cooling devices for PEMFC systems and was testified here for an air-cooled FC stack.

A 3-dimensional flow simulation was created by S. Shimpalee and S. Dutta [4] to study the numerical analysis of the flow channel. This numerical model assumes steady state and multiphase behavior of the flow channels. The Important finding of this paper is that the performance of fuel cell not only depends on inlet set-up conditions like membrane thickness, inlet flow rate, cell voltage but also temperature variation inside the fuel cell model. Nguyen et al. [5] proposed a two- dimensional model with steady-state, two-dimensional heat and mass-transfer. The model was used to gauge the effectiveness of various humidification strategies.

The results confer that the anode gas stream must be humidified before letting into the fuel cell as the back diffusion of water is insufficient to maintain the membrane hydrated. This enables us to study the operating criterion on performance of the fuel cell to model cell design for a specific utilization to regulate a fuel cell.

Matian et al. [6] developed a computational model of the PEM fuel cell to study the heat generated and distribution of heat of the surface of the model using thermal imaging cameras. Two models, single-cell and two-cell stacks, with a focus on temperature divergence on the external and internal surfaces of the stack under different loads were studied. The Validated results showed that the temperature distribution in a stack is influenced by stack composition and drawn power density. Hence, there becomes a very high implication for better thermal management in FC stacks with large number of cells.

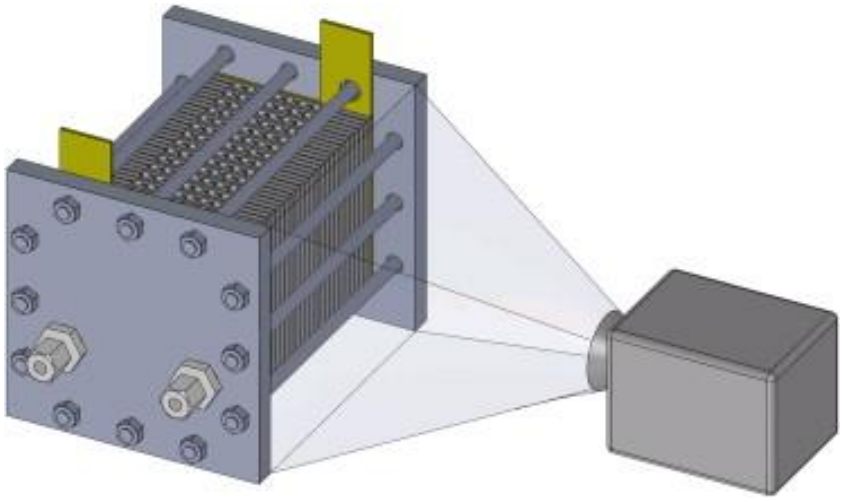

Figure 2: Thermal Imaging Camera Technique [6]

Alejandro et al. [7] provided key inputs to develop powerful model and validate the obtained results through a dynamic system (1.2 KW NEXA) which is very commonly used by research groups. The model proposed semi-empirical formulation, theoretical and experimental data combined together. The main contribution of this model is unique way

of obtaining polarization curves experimentally, and modification of the thermal equations for an air cooled stack and modeling of flooding event in the FC stack. The heat distribution on the surface of the stack is very difficult to measure experimentally because of complexity of heat and water interaction. [8] Design consideration for PEM FC is a key factor while taking into account catalyst particles, GDL (gas diffusion layers) and bipolar plates, to integration of the fuel cell stack with various external subsystems.

Djilali et al. [9] analyzed the fundamental modeling of specific transport phenomena encountered in component Layers of MEA. The MEA consists of a proton exchange membrane sandwiched between catalyst and GDL. Moreover, discussed the integration of some of PEM FC models into multi-dimensional CFD codes and illustrated their application in plate and frame unit cells. Sharifi et al. [10] analyzed the performance of a fuel cell as a function of voltage – load current characteristics. In this regard, two complete fuel cell models under steady-state and dynamic conditions were proposed. The steady-state electrochemical model for PEM fuel cells was presented. Transient phenomenon in this paper combines together simultaneously three prominent dynamic aspects like temperature changes, Fluid flow and pressure changes through channels of double layers. Yi Zong et al. [11] proposed a non-isothermal and non-isobaric model with non-uniform stack temperature. The model consisted several parts like mass balance, energy balance, pressure drop and cell output voltage. The mass balancing equations are used to calculate the energy balance equation and Newton–Raphson method is applied to calculate the local current density. Based on the simulation on both anode and cathode, it was found that anode and cathode should supply with humidified fuel, to prevent the

membrane from dehydrating. Also, it was found that the flow pressure increases the performance of the FC.

Bao et al. [12] established a one-dimensional, steady state, isothermal FC model that focused on design methodology and analysis of water and thermal management of the FC. More recently, Cao et al. [13] developed a three dimensional two phases, non-isothermal model of the PEMFC to perceive the interaction between water and heat transport, fluid flow of the model, electrochemical reaction and heat transfer process. Musio et al. [14] established a modeling approach which was implemented in Matlab-Simulink context. The stack model was set up based on elementary equations for fluid dynamics, thermal dynamics and kinetic behavior of the system. A thermal control model for the system was progressed for an air cooling system which enabled in differentiating various heat removal strategies. Finite differencing (FD) have been used to understand the heat transfer mechanism. For instance, Mayyas et al. [15] associated a 3D model using FC heat transfer technique correlated with experimental boundary conditions for hybrid power train containing battery pack and power electronics. The model predicted the spatial and temporal temperature portrait in accord with the actual vehicle conditions. Similar, approach is used in this study, but in this case the subject of study 3D fuel cell model.

2.2 Apparatus used

NEXA 1.2 KW fuel cell System

The Nexa FC system provides simulated non-regulated output voltage of the fuel cell system to 24/48 V DC voltage and enables battery hybridization. The Nexa OSC software provides overall efficient control of the Nexa1200 system. The entire data from all

attached components could be centrally parameterized and controlled. Figure 3 shows the image of the fuel cell system.

Figure 3: 1.2 KW NEXA fuel cell

The NEXA 1.2 KW fuel cell has FC GEN 1020 (BALLARD) stack stationed in it. This stack has been engineered to integrate advanced open cathode technology where the inlet air is inherited from the atmosphere. The state of the art technology has instilled with a self humidifying MEA (membrane electrode assemblies).This expedites the water piled up during the reaction, to evaporate amidst the cooling air and is blown out by means of the air duct at tail of the system [16]. The primary advantage of the FC gen 1020 is that it could be scaled from 300 W to 3 KW easily and also integrated with other application user. The stack is placed in tilted position to facilitate the air inlet and cooling the system. The NEXA system has maximum power capacity of 1200 W and current of 52 A. The investigated FC stack is packed with 36 cells.

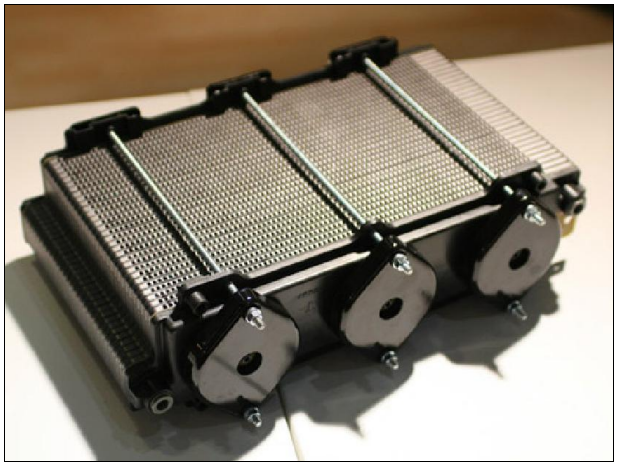

Figure 4: FC gen-1020 stack

Moreover, the FC has an in-built new software experimentation and data acquisition measurements. This provides a consistent status of the system with flow rates, current and power drawn. Figure 5 shoes the data acquisition window.

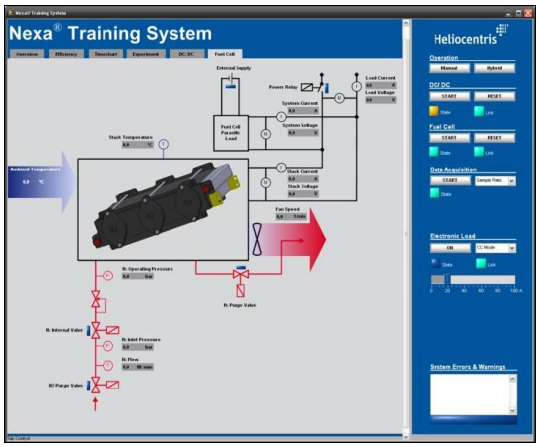

Figure 5: NEXA data acquisition Window

PXI 1071Controller

PXI 1071 Controller is a state of the art measurement based platform advanced by National Instruments (NI). This has an in-built X series data acquisition capable of providing 16 analog inputs and 2 output signals. This typically controls the load profile

drawn out the FC system based on the loaded input signals created through the artificial drive cycles.

Figure 6: NI PXI controller

The controller is capable of dedicated bandwidth of up to 1 GB/s per-slot x4 PCI Express), while the total system bandwidth of about 3 GB/s. The controller uses two Data acquisition systems namely the PXIe-6341 and PXI- 6722 controllers. The PXIe-6341 was used to communicate with the e-load to draw the load current.

DC Electronic load:

The DC e-load used here is the AMREL PEL 300-60-60. This is a programmable real time DC load which is an important criterion to be met for. The power capacity here is around 300 W. The power is drawn out by the FC as per the load requirements as dynamically controlled by the PXI controller.

Figure 7: AMREL DC e-load

Thermal Imaging Camera

Thermal Imaging is proved to be an effective technique for diagnosis of operating fuel cells and fuel cell stacks. In this case, we use T620 FLIR camera for imaging purpose. Figure 6 shows the thermal camera. It can be used to identify variety of phenomena that are associated with non-uniform generation of heat. [17]

Figure 8: Thermal imaging Camera

The specifications of the IR camera are illustrated in table 1. The camera also comes with a FLIR Viewer app to import thermal images from the camera, add more box areas and fine-tune images. Furthermore, this also enables us to generate detailed reports of the images obtained.

Model Name	T620 FLIR
Camera Resolution	307,200 pixels (640 × 480)
Field Of View (FOV)	IR FOV
Temperature range	-40 to 650°C
Spectral Range	7.5–14 µm
Data Plotting Software	Examin IR 1.40.2
Thermal sensitivity	< 0.04 °C at 30°C
Frame Rate	30Hz

Table 1: IR camera specifications.

Thermo-couples (K-series)

The thermocouple is very widely used component for measuring temperature across any part or area. In case we have used the K-type as they possess the widest operating temperature range. Moreover, they work for all applications as they are very stable and possess high corrosion resistance.

Figure 9: K-type Thermocouple

The two K type thermocouple network (one at the center and another towards the periphery) was instilled on the surface of the FC stack to record the temperature variation for each artificially induced drive patterns.

Software set up and driving Cycle

The concept of performing HiL configuration and modeling were accomplished using MATLAB/SIMULINK©. This is an advanced software platform developed by Math works. **[18]** This enables to provide block diagrams for several mathematical operations for simulation programs. This is one of the most efficient methods to drive the Matlab program. It's widely used for testing purposes for dynamic modeling.

The inputs to the SIMULINK models are given in form of standard pre-defined cycles. These drive cycles were established by different counties based on the road conditions to that particular region and standard drive profile**.** The drive cycles were used to judge the several vehicle performances such as the fuel economy & consumption, emissions etc **[19].** Three driving cycle patterns based on the US Environmental Protection Agency (EPA) **[20]** were used. These were formulated to by the agency to various types of

automotive systems. These drive patterns are used all over the world for testing the vehicle parameters.

The features of the driving cycles are discussed in table 2.

Driving Cycle	*Features*
Federal Urban Driving Schedule (FUDS) or Urban Dynamometer Driving Schedule (UDDS)	• Symbolises the driving profile of a city. • Maximum speed limited to 55mph
Federal Highway Driving Schedule (FHDS)	• This is highway fuel economy test • Represents a highway drive scheme • Maximum speed limited to 60 mph
US06 driving schedule	• Also known as supplemental FTP (Federal Test Procedure) • This is a more aggressive representation of city driving profile • The Maximum speed goes up to almost 70mph
Acceleration Test	• Custom made test which runs for 100 seconds and draws maximum current from the FC system.

Table 2: Driving cycle specification

CHAPTER THREE

3. METHODOLOGY

3.1 Experimental Set up

This section provides the fundamental procedures and mechanisms required to establish a prototype and attain the required boundary conditions from an operating Fuel cell system (FC). This empirical work helps to get stack temperature, stack voltage, flow rates, net power and temperature distribution on the surface of the stack.

The experimental set up consists of NEXA 1.2 KW fuel cell (Heliocentris), PXI 8102 controller, AMREL DC electronic load and IR Forward looking infrared (FLIR) camera. The NEXA 1.2 KW fuel cell has FC GEN 1020 (BALLARD) stack stationed in it, as illustrated in figure10. This stack has been engineered to integrate advanced open cathode technology where the inlet air is inherited from the atmosphere. The state of the art technology has instilled with a self humidifying MEA (membrane electrode assemblies).This expedites the water piled up during the reaction, to evaporate amidst the cooling air and is blown out by means of the air duct at tail of the system**.** The stack is placed in tilted position to facilitate the air inlet and cooling the system. The NEXA system has maximum power capacity of 1200 W and current of 52 A. The investigated FC stack is packed with 36 cells.

The PXI 8102 Controller function as hardware-in- loop, which infers input from simulated FCV model. The entire FCV consisting of FC system is advanced using Simulink (MATLAB). The inputs for the Simulink model are the devised standard drive cycles. The PXI controller simulates the drive cycles through the AMREL DC electronic load, which extorts current from the FC system, based on the input signals. AMREL 300

W PEL series 300-60-60 DC electronic load is used as a power plunge for the FC power. This is a manikin load which systemizes the power drawn from the fuel cell. This load draws from the FC based on the drive cycle signals sent from 8102 PXI controller.

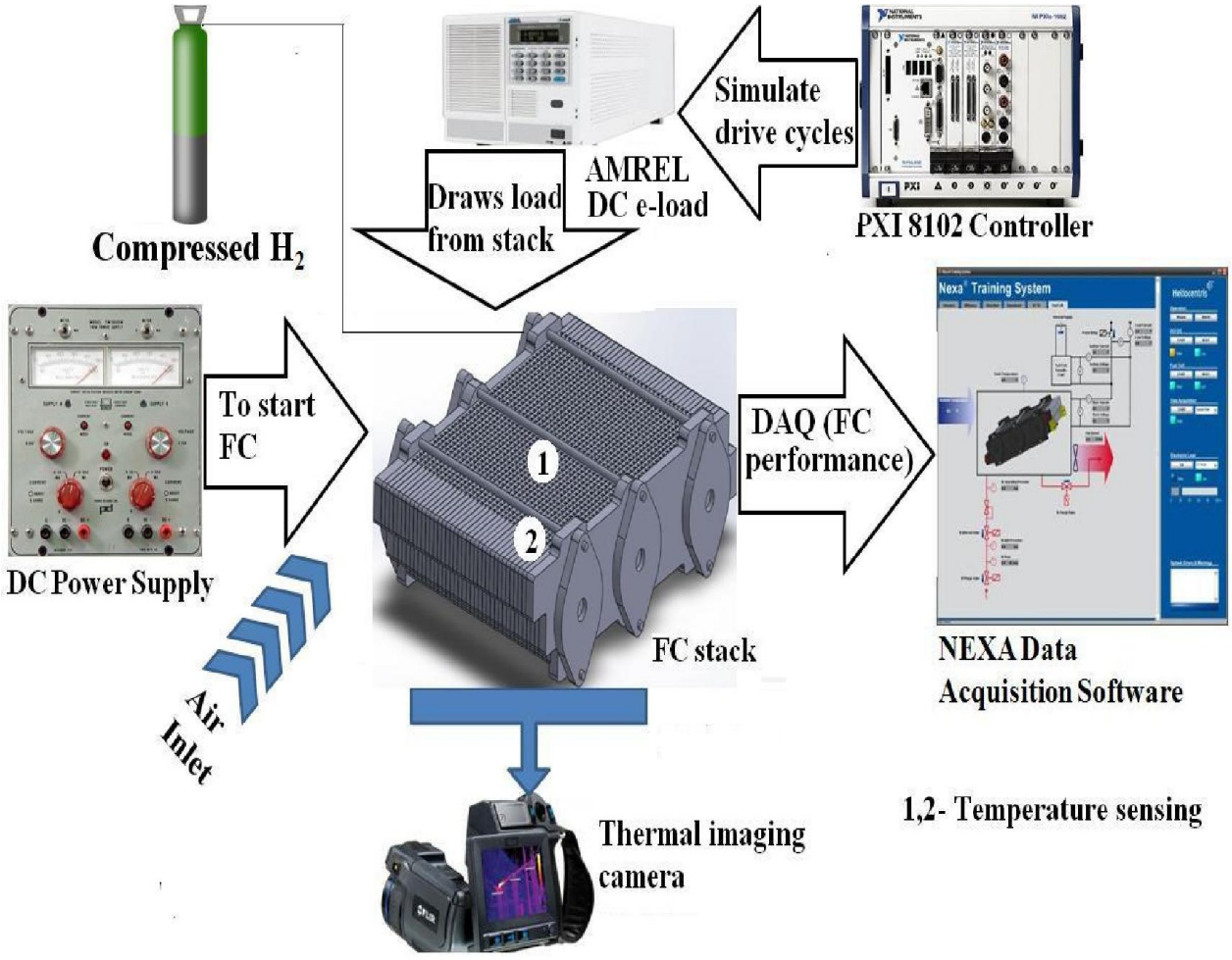

Figure 10: Schematic of the experimental set-up

The Fuel cell is connected to 3650-S DC power supply manufactured by Power Designs Inc. The power supply initiates the fuel cell system at the beginning of operation.

3.2 Experimental operation

The thermal performance of the 1.2 KW FC systems is surveyed under several transitory conditions for different power requirements, operating under different standard and user defined drive cycles. The entire FCV consisting of FC system is advanced using

Simulink. The inputs for the Simulink model are the devised standard drive cycles. The input signals for the Simulink model includes three standard drive cycles Federal Urban Driving Schedule (FUDS), Federal Highway Driving Schedule (FHDS), US-06 (Aggressive urban) and Acceleration Driving Test (ADS). This mix of city, highway and aggressive driving patterns replicate a real-world driving condition. The speed profiles are fed to the Simulink model in real-time. The model and based on the torque command will dictate the power demand in real-time to force the DC power supply draw the necessary current from the fuel cell. These scenarios are more practical approach in studying the performance and analyzing the behavior of the fuel cell in HiL configuration.

The FC current, Flow rates and voltage are obtained for each standard drive cycle. The electric current and voltage of the fuel cell is scripted at one Hz based off the drive cycle with an in-built data acquisition system. The DAQ keeps a log of FC stack voltage, load current, FC temperature, operating pressure and ambient temperature at one Hz through various drive cycles.

The structural and terrestrial temperature contour for FC stack is documented for various drive schedules using an infrared detector. A FLIR T620 focal plane array FPA Thermal Imaging IR Camera was placed in front of the FC stack at a distance of about 1 m to capture the 2D superficial temperatures in real-time. The camera is also equipped with Examin IR 1.40.2 real-time image/data logging and plotting software as already discussed in the Apparatus used section [17]. The thermocouple network was positioned to detect the temperature divergence on the surface of stack. The thermocouples are

critical as they complete the closed loop feedback system, transmitting signals to PXI controller.

The FC system assessment began at 23 ^{0}C, in a sequential manner with FHDS cycle simulated first, followed by FUDS, US-06 and at last ADS. This systematic approach of drive cycle simulation helps us to study the fuel cell in steady state condition in more meticulous manner. Federal Highway Drive Schedule (FHDS) and Federal Urban Drive Schedules (FUDS) represent drive cycles used by U.S. Environmental Protection Agency to validate that light duty vehicles fulfill the federal emissions and fuel economy standards as already discussed in the previous sections. This helps to study the rapid heating of the surface mount on FC stack at extreme loading conditions.

3.3 3D Model analysis

It is always a general practice to build a 3-D model of any prototype to analyze the problems in design process. In this manner we avoid any expensive prototype build up. Furthermore, this would enable us to makes any design refinement. Therefore, this enables us to shorten the design time and cut down unnecessary expenses. [21]

Generally there are four steps for a thermal model to be developed

- Generate the surface and mesh them
- Define the material properties and boundary conditions
- Perform the analysis
- Post process the results

The FC model was created in solid works as per the measured dimensions. This was typically duplicating a single cell into as many as 36 cells. Once the surface geometry

was created, the parallel flow field was constructed across the model as shown in Figure11.

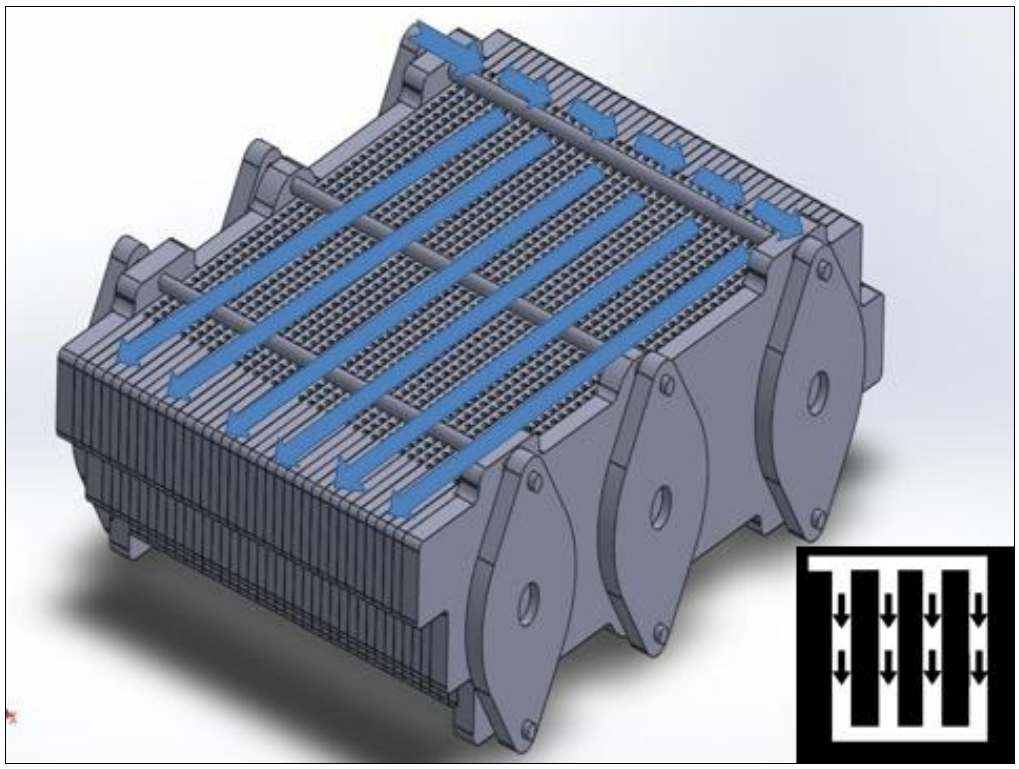

Figure 11: 3D FC model with flow pattern

This surface geometry forms the base for thermal model. [22] So it becomes prime importance to construct the model carefully without any unconnected vertices or irregular shape. The 3 D model is required to be meshed with a precise quality to perform accurate thermal analysis in the Finite Differencing Code (FDC).

3.4 Meshing Criteria

Meshing is a process of discretizing a surface into several smooth surface polygons. This could be used for variety of applications. The surface Finite differencing purposes, triangles and rectangles are preferred. But the volumes are subdivided into tetrahedral and hexahedral.

The mesh generation for thermal model is critical task, which requires modeling expertise and high quality tool. [23] This is not a liner process. Mesh creation begins with the existing model to produce quality thermal model. The 3D model of the complete FC stack is required to broken down to FE model to improve the precision of the analysis.

The mesh size is always a question for ages, the smaller the mesh, better the mesh. But there is a problem of solve times. The aspect ratio i.e. length to width is always < 4.0, to guarantee for even lateral flows between the connected vertices as illustrated in Figure12.

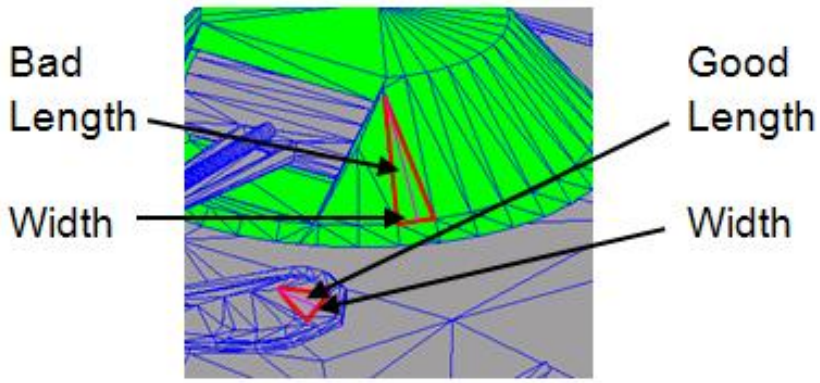

Figure12: Aspect ratio of Meshes

The triangles and quad elements (5-25 mm or larger) were used to resolver thermal spatial geometry and gives very good convergence criteria. Also the surface is broken into several parts and materials with a thickness ratio less than or equal to 0.5mm. The quad elements are best suited for thermal analysis. Besides this triangles can also be performed for all curvature parts and profiles. But the important point to be noted is the vertices must be connected for face to face conduction. It also required making sure that the vertices are connected properly. This is to make sure that there is proper conduction as shown in figure 13.

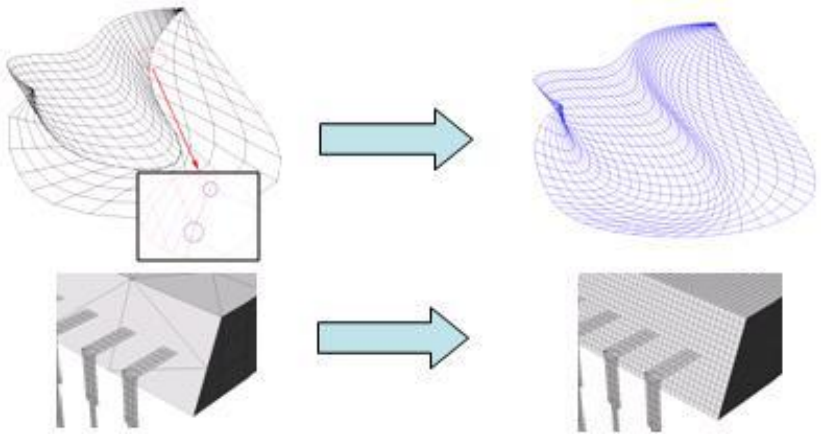

Figure 13- Conduction problem (Unconnected vertices)

Meanwhile, the war page of the planar measurement should not exceed 4-5 degrees as shown in figure14 [24]. Some of the other criteria to be carefully noted are the connectivity, overlapping and penetration for the radiation elements.

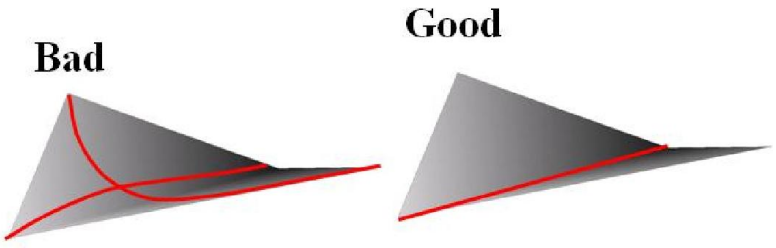

Figure 14: War page- Planar measurement

As an overall process, quality, size and Skewdness of meshes of the 3D part are critical part in simulating the three dimensional models in the FDC thermal solver. FDC corresponds to give better results with respect to the quality of the meshed. This is due to the fact that FDC assumes a centroid based calculation for the thermal analysis as shown in Figure 15. To add to this, proper meshing depends on the complexity of the model under study. The density of the elements in terms of giving fine or course meshes depends on the level of thermal analysis. [25]

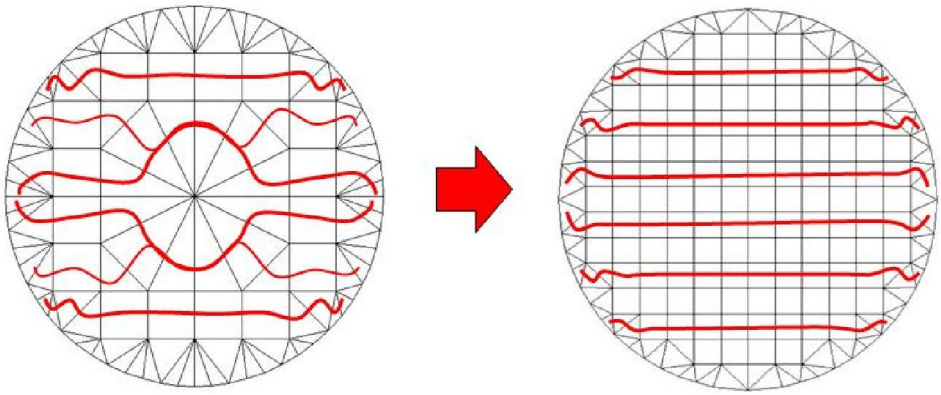

Figure 15: Centroid based calculation

Using ANSA meshing tool from Beta systems; the CAD geometry of the complete fuel cell model was meshed, cleaned, repaired; and imported into RadTherm software (Thermoanalytics Inc). Nevertheless, to make easy the process and reduce the simulation time of the FE model for a complete FC, the stack was the main point of consideration. Figure 16(a, b) illustrates the complete FE model of the complete FC and FC stack.

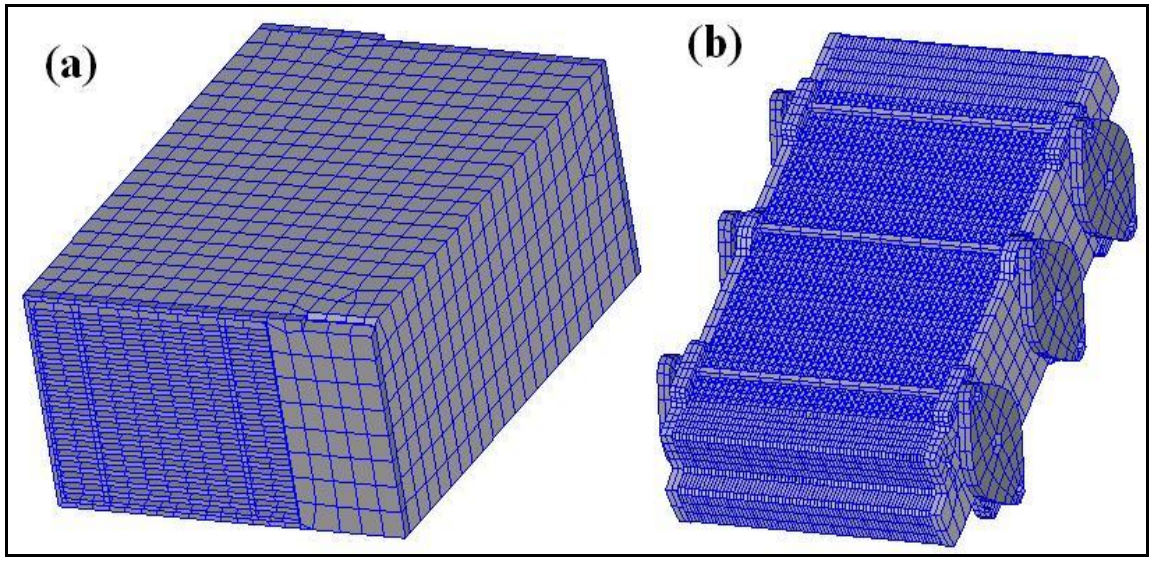

Figure16: FE model of (a) complete FC (b) stack

3.5 Simulation Tool

One of the most current thermal simulation tools based on FDC-Radtherm was used for thermal modeling and analysis. This software package has an optimized thermal solver to provide 3-D thermal model the user interaction and also an image viewer (wireframe and animated thermal display).

The software has the competence to resolve to the steady state and transitory heat approach. Radtherm can import element, alter the geometry properties of elements or group. More importantly, the solver is capable of breaking each part of element into thermal nodes. In FDC, the generated 3D model is designated with the attributes for each of elements or cluster having same thermal attributes with thickness, emissivity, flow rates, direction of flow contrast to time curves. The FDC splits the elements with same properties into thermal nodes. The total radiation exchange between two surfaces which are assigned to different thermal nodes i and j is calculated using the equation *(1)*

$$Q_{ij} = B_{ij} A_i \varepsilon_i \sigma_i (T^4_i - T^4_j) \quad \text{- (1)} \quad [26\text{-}27]$$

Where Q- net radiation heat exchange in Watt

B_{ij} - energy emitted from surface i and absorbed at surface j both directly and by reflection

A- area in m^2

ε_i - emissivity,

σ_i - Stefan–Boltzmann constant in Wm^2K^{-4}

Ti, Tj - temperature of objects i and j respectively in Kelvin.

One of the key factor and advantage of the existent solver is its ability to create thermal nodes while replicating fluid streams. Though, the solver calculates the temperature

nodes based on practical mode, the theoretical way of calculating node temperature is by an energy balancing equation given by *Equation (2)*

$$\sum Q^{*} = m.C_p\,(dT/dt) \text{ - } (2) \quad [28].$$

Where Q is heat rate in joules, m is mass in kg,

C_p is the specific heat,

T is the temperature in K.

Following, the solver calculates the viewing factors by iteratively distributing the objects as it is linked by the thermal nodes. The obtained image has each pixel loaded with some data, adding up all pixels corresponds to same thermal node. [29] This is the prime reason why the FE mesh produced is to be concurred with the solver which chooses the centroid of each element at which the view factor is calculated. It is to be noted that the convergence factor defines the temperature difference for thermal node of the present and following iteration in this case the solver utilizes 0.01 to 0.001 ^{0}C subjective. Additionally, the multi-layer surfaces are denoted by a grid of nodes spatially well defines within the same layer. Figure 17 illustrates the graphical user interface for RadTherm solver.

The most key factor of this solver is that it allows us to establish the thermal nodes and fluid streams which are the most important criteria for any thermal model. Because of the fact that the solver does not conjoin the fluid streams in one bounding part, a necessary breakdown for parts simulating them precisely. [25]

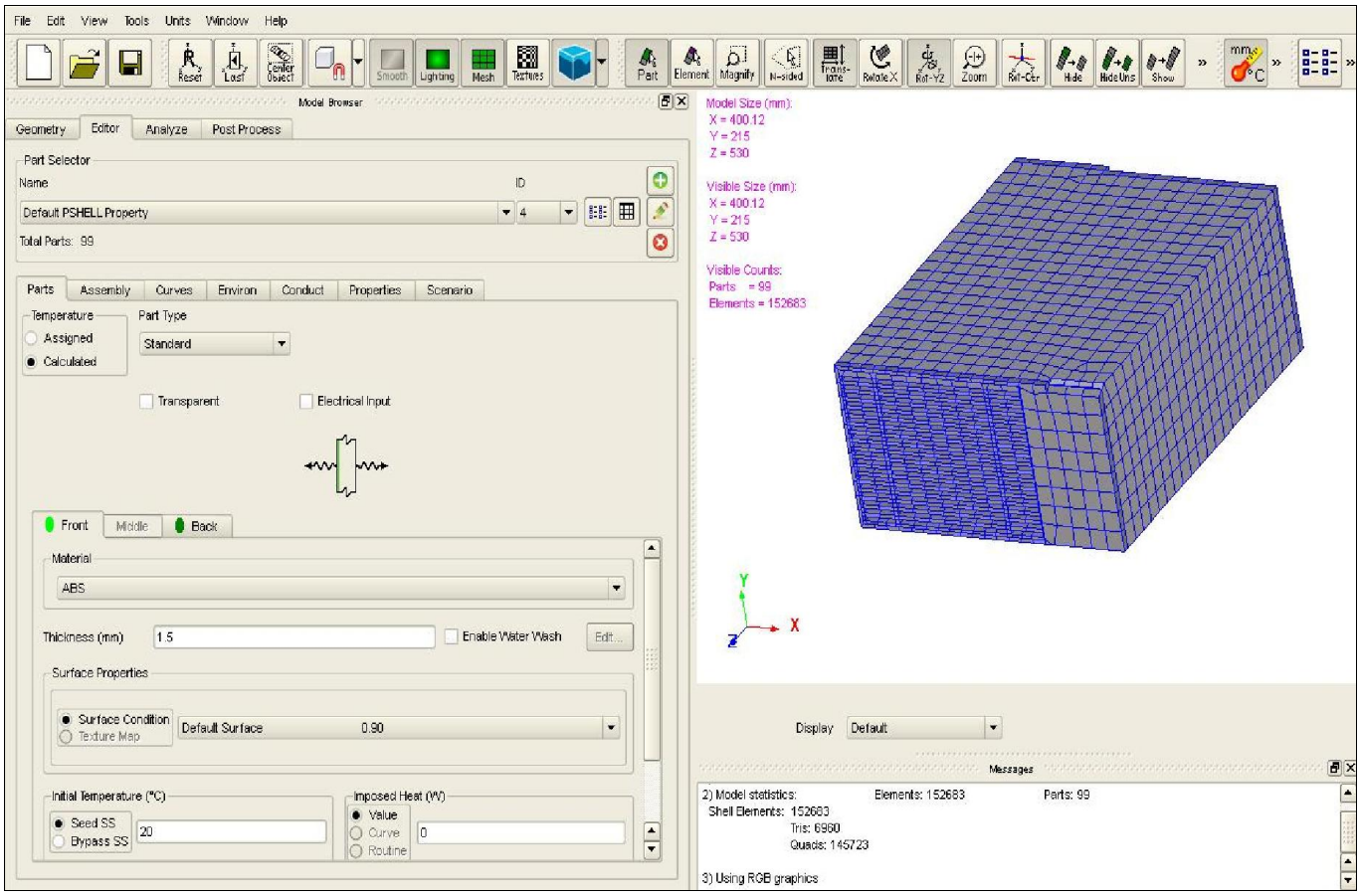

Figure17: RadTherm Graphical User Interface

Material properties, surface conditions, initial temperature were established for each cell and also other parts of the system. Fluid streams for inlet hydrogen, intake air, stack cooling fan speed were assigned and ringed with its connected geometrical parts.

3.6 Current, Voltage, Flow rate analysis

The FC current, Flow rates and voltage are obtained for each standard drive cycle. The electric current and voltage of the fuel cell is scripted for every second of the drive cycle with the in-built data acquisition system (commercial name DAQ). [30] The DAQ keeps a log of FC voltage, FC current FC temperature, Operating pressure, ambient temperature and system current for each second of operation through various drive cycles. It is noted that there is always static current of 1.43 A drawn from the FC stack, this is the current

derived by the electronic components of the FC system for its manipulation. But the maximum flow rates for hydrogen and air is given based on the Stoich on the anode and cathode respectively.

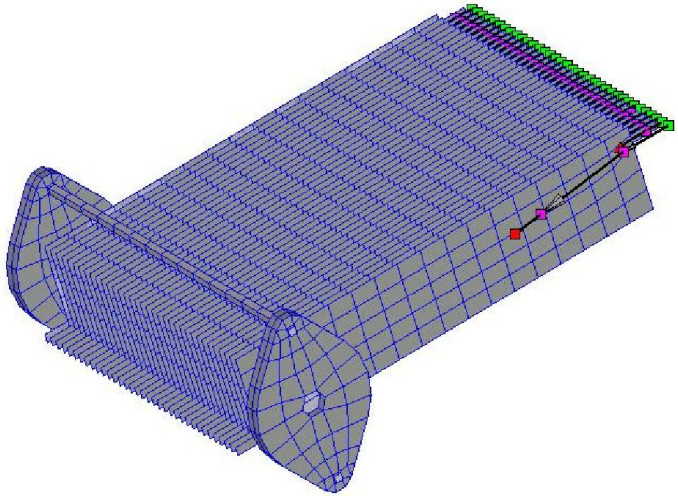

Figure 18: Fluid streams across the FC stack

The maximum Flow of hydrogen (anode) is given by,

Anode Stoich =1.1, Maximum current FC= 52 A

7 SCCM of Hydrogen produce 1 A current

So the maximum Flow= 52*1.1*7 = 400.4 SCCM = .4004 L/min per cell

The maximum Flow of air (cathode) is given by,

Cathode Stoich = 5, Maximum current FC= 52 A

16.66 SCCM of Air produces 1 A current

So the maximum Flow rate= 52 *5*16.66 =4331.6 SCCM = 4.331 L/min per cell

1000 SCCM= 1 Liter

The Fluid nodes were initiated to link the fluid stream inlet to split into the channels for each cell as illustrated in Figure 18.

The cooling fan mechanism determines the corresponding cooling and inlet air mass flow rate; with the intake air quality is combined with the chamber surrounding. Similarly, fluid nodes were created for air inlet to connect the model front side with ambient air through the cells, in a way to fabricate forced convective heat transfer between the stack flow field and the ambient air. The created fluid node is linked with every cell in 36 cells stack, to replicate the fluid inside the stack. A temperature curve obtained from two pre-existed thermocouples discussed earlier is also designated to a fluid node within each cell. The solver is run for each drive cycle in order of sequence, to replicate the heat transfer for the FC components. The simulated results are compared with the thermal images obtained from the Exam IR (FLIR camera software). This helps to analyze and study the hotspots and thermal maps on the surface of the stack. The following section talks about the temperature measurements.

3.7 Temperature Measurements

There are two temperature measurements devices used namely IR camera and thermocouples. The Infrared detector is a non-contact temperature measurement feature. This is actually based on radiation\emissivity which makes this as a time responsive tool. Moreover, this is a high durability and non-contamination. [31] This also accommodates all materials since the all of them emit or conduct heat. The structural and terrestrial temperature contour for FC stack is documented for various drive profiles using a thermal camera.

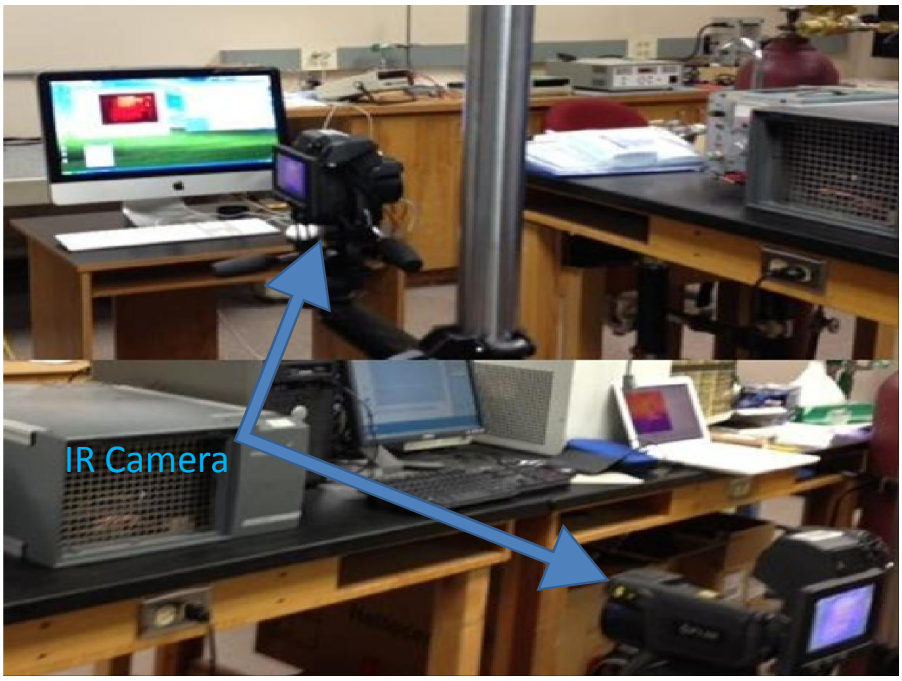

Figure19: IR camera set up

There are several criteria's which needs to be fulfilled for effective use of the thermal camera. For example, the thermal detector needs to be insulated from any external forces like the dust or any other particles which might disturb between the space between the camera and the target source. [32] The target source should always be in the FoV (Field of View) of the camera to avoid any hindering object which might cause temperature interpretation. It is also necessary to understand that the target should be twice bigger than the area of interest or study. But the range of the IR cameras is subject to operating temperatures which may cause an improper temperature measurement if it's exceeding. [33]Another important factor is to note the emissivity of the target source [34, 35]. The emissivity of the measurement depends on the surface of the target. Typically the emissivity of components was either measured or obtained from the manufacturer's data. In case of calibrating the IR detector, the black body method was used to obtain accurate temperature data.

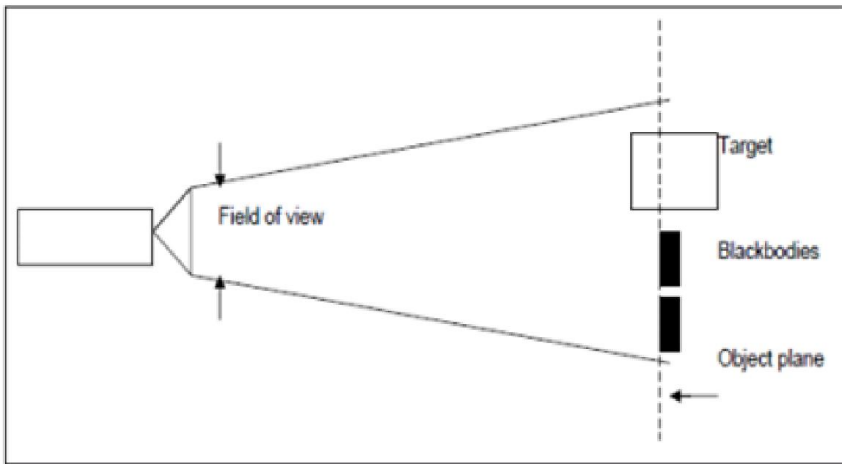

Figure 20: Calibration using black body method [22]

In this case, the thermography camera was employed using a dual band to neutralize the emissivity for various dynamic ranges to obtain accurate surface temperature of the FC stack and its components. The FLIR T620 used in this scenario is a cooled infrared detector which easily measures the temperature of the hotter parts of the target (FC stack). The specifications of the camera were already discussed in the second chapter. The surface temperature of the FC stack was captured over for all 4 standard and artificial cycles with the speed variations from 10 mph to 80 mph.

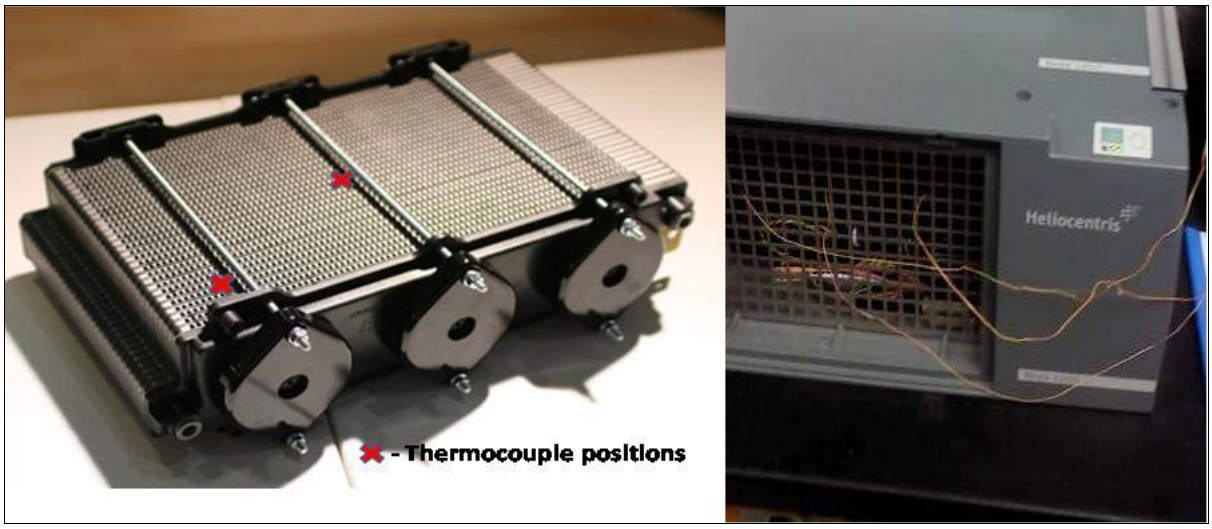

Figure 21: Thermocouple positions on the FC stack

Additionally, a thermocouple networks are installed at two different locations on the surface of the stack to provide a reference signal and temperature at particular locations. Figure 21 illustrates the discrete positions at which the thermocouples where slotted for temperature measurements. The thermocouple network is positioned to detect the temperature divergence on the surface of stack. The thermocouples are critical as they complete the closed loop feedback system, transmitting signals to PXI controller. In each experiment as pre test practice, the ambient temperature was measured for preparing the surface of the part for the test. Moreover, there is another thermocouple which is just left in free space to measure the ambient or room temperature. The thermocouple are attached are carefully attached to the surface of the stack using a thermal tape. This tape acts as a coupler which fills the gap between the surfaces without conducting heat.

CHAPTER 4

THERMOELECTRIC MODULES

4.1 Introduction

A Thermoelectric cooler, TEC, operates on the Peltier principle. This principle is the presence of heating or cooling at an electrified junction of two dissimilar conductors [36]. In the work described here, Peltier cooling is utilizes as a mechanism to control the incoming air temperature. The Thermoelectric coolers (TEC or Peltier) has a capability to create a temperature differential on each side of the module. [37] One side becomes hot and the other side gets cold. Thus, this shows that it could be either warm or cool something, based on the operation required. [38] This temperature differential can be used effectively to generate electricity. The rate that the Peltier heat is liberated or rejected at the junction (Q_P) is given by:

$$Q_P = \acute{\alpha} IT$$

Where, I is the current through the junction and T is the temperature in Kelvin.

The TEC works very well as long as the heat is removed from the hot side. Once the device is switched ON the hot side heats up quickly. If the heat is not removed from hot side quickly, the device reaches static and does nothing. Some of the TEC models and heat sinks are illustrated in figure 21.

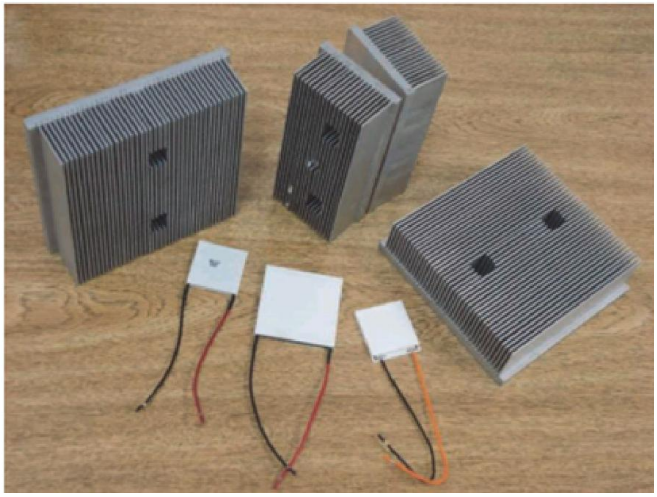

Figure 22: Thermoelectric models and heat sinks [36]

The thermoelectric module consists of p-type and n-type semiconductors elements which are heavily doped with electrical current carriers. These elements are connected electrically in series but thermally connected in parallel. These charge carriers are affixed on each side of the elements i.e. one covers the hot and the other covers cold side. [36]

The thermoelectric devices offer several advantages over other technologies, the major advantage being the absence of moving parts, low maintenance and high reliability. The absence of working fluids, dangerous leakages and low noise makes it perfectly suitable for our application purpose. A special aspect of TE conversion is that the energy flow is reversible. So instance, if the load resistance is pulled out and a DC power supply was substituted the TE modules can draw heat from the heat source. In our configuration, the energy conversion strategy is conjured using electrical power to pump heat and produce cooling. This unique character distinguishes this from many other conversion devices. Any Thermoelectric module can apply for both modes for operation by optimizing them for specific purpose.

4.2 Working Principle

The TEC is considered as an exceptional cooling technique enforced to thermal operation in PEMFC to cool the bipolar plates [25]. The FC model is compounded with a custom-made thermoelectric cooling system. The system consists of an air duct with internal fins extruding towards the center, and thermoelectric modules mounted on the outside of the duct. As electrical current flows through the thermoelectric module, the current-induced phonon transport in the "π-junctions" in the module allows for heat to be removed from one surface (the cold-side) of the TE module, and ejected through the other (the hot side). The hot-side of TE module in this system is attached with fan to allow removal of heat ejected from the module, while its cold-side is mounted on the outside of the cooling duct to allow removal of heat from the fins as illustrated in Fig. 11.

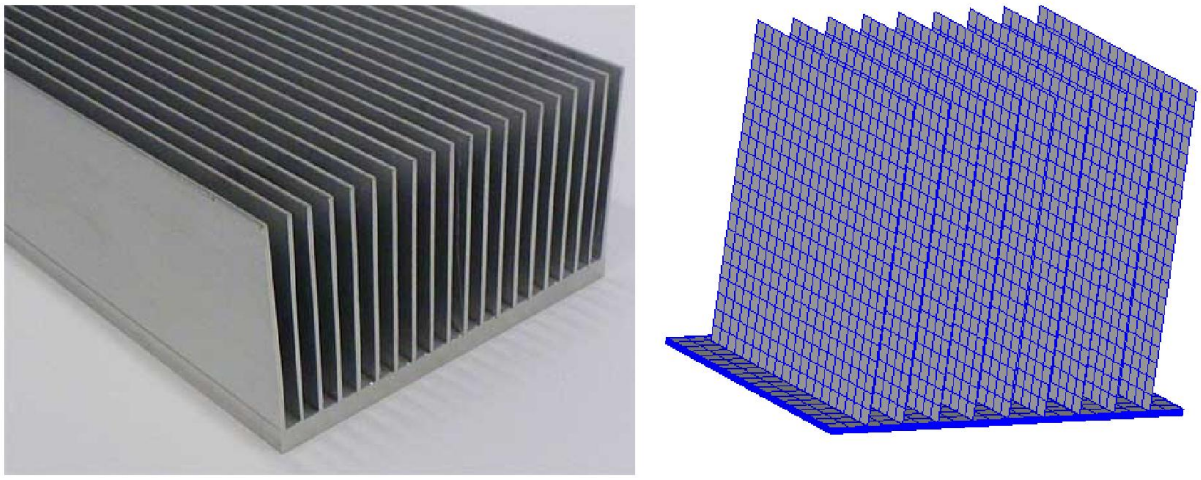

Figure 23: Thermo electric Module with fins

As the incoming air flows through the fins, it cools down by losing heat to the fins. Since the duct with internal fins is an integral part of the thermoelectric cooling system, the design and selection are very important. The system also includes an air temperature sensor and a temperature control loop to ensure the optimal air temperature is maintained.

This model is specifically tested for the Acceleration Drive Schedule (ADS), as this drive cycle manifests greater thermal signature.

CHAPTER 5

RESULTS & DISCUSSIONS

5.1 Model Validation

In order to verify the complete 3D thermal model of the Fuel cell, the outcome of the model runs for each standard drive cycle was retrieved and validated with the outcome for a real test run. Thus, the transient and a spatial temperature plots for the FC stack obtained and compared with the actual temperature curves. In Addition to this, the incident, outgoing and net heat rates through conduction, convection and radiation for the elements were used. This was performed to evaluate the efficiency of the air cooled system of the FC stack. The front and back temperatures of the FC stack were studied to understand the effect of heat generation the chemical reactions and its effect on cell degradation. Furthermore, the thermal performance of the FC stack with and with Thermo-electric modules under the standard and artificial drive cyclic loading was analyzed.

5.2 FC simulation results

Following to a lucrative retrieval of the boundary conditions with the help of the available data from the test run, the fuel cell model was run for each of the driving cycles applied in the test (FHDS, FUDS, US-06 and ADS), while the time duration for enforcing the thermal solution was set with respect to the time limit of the drive cycle being simulated with 1min time step size. The thermal performance of the fuel cell was observed under transient and steady state conditions by positioning two locations on the surfaces of the FC stack (one cell in the middle and another at corner of the FC stack).

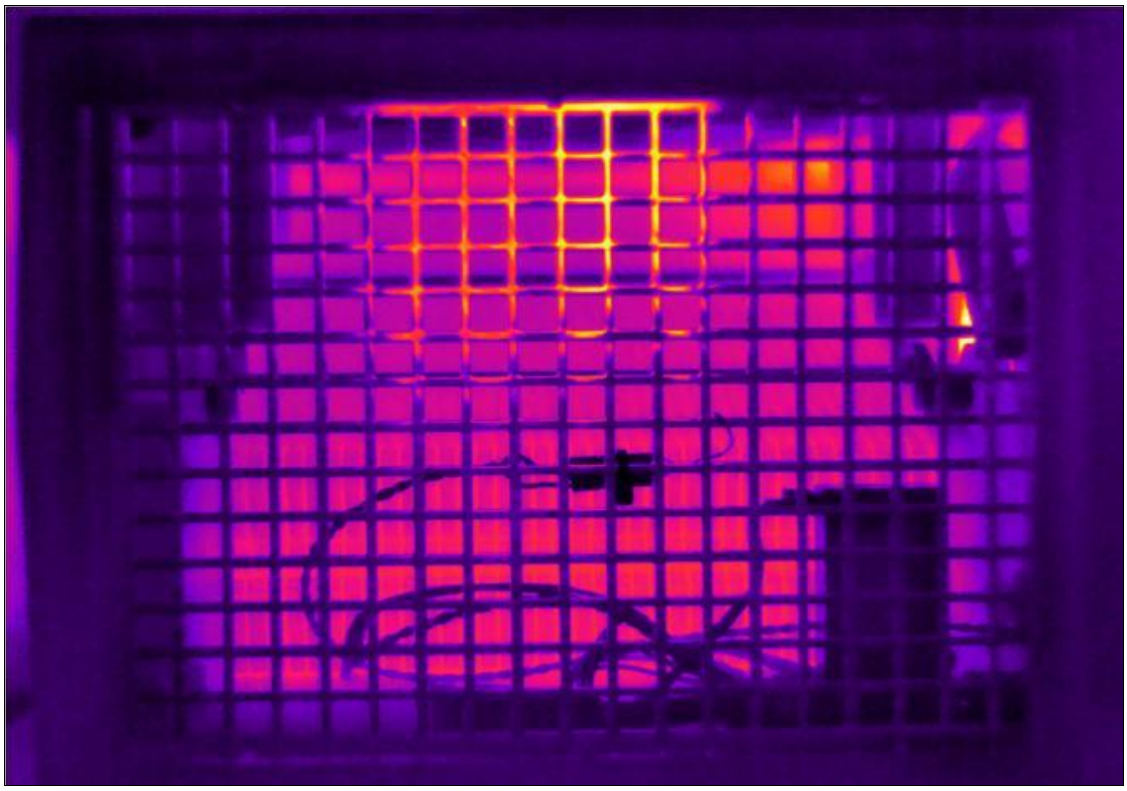

Figure 24: Net heat flux as predicted by Thermal camera

As the IR detector provides the 2D spatial and transitory surface temperature contours, a contrasting comparison was performed with the net heat flux as predicted by the thermal model. Figure 24 and Figure 25 illustrates the net heat flux across the FC stack as predicted during FHDS by the thermal camera and thermal model respectively.

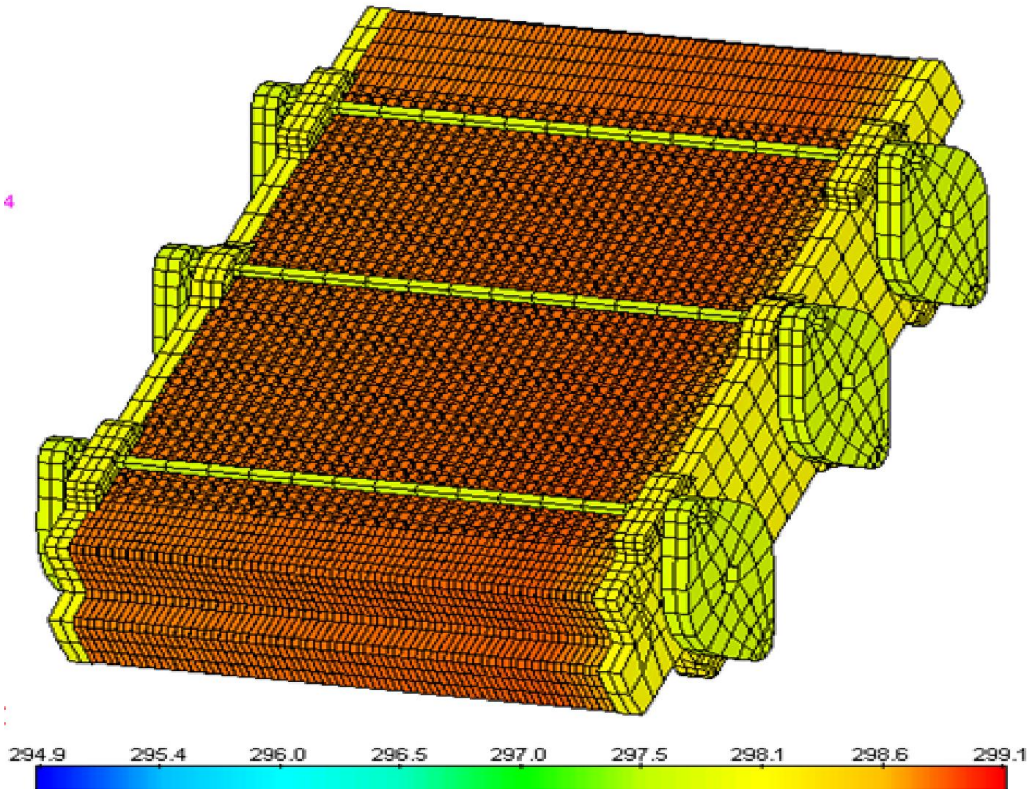

Figure 25: Net heat flux as predicted by 3D Thermal model

It is evident from the image that middle of the FC stack is more heated up than the sides or edges of the stack. This suggests that the heat gradient is more towards the center of the stack. Moreover, the cells away from the center are better capable of transmitting the heat to atmosphere by conduction, convection and radiation. Further, the cells at the middle of stack experiences similar load fluctuations and radiate same heat as the edge cells. This shows the chance of heat transfer to the neighboring cells is almost due the fact that there is no temperature variation. To retrieve a better picture of the heat fluxes through the stack, figure 26 displays the cells heat propagation at the end of US06 drive cycle test as predicted by the thermal model.

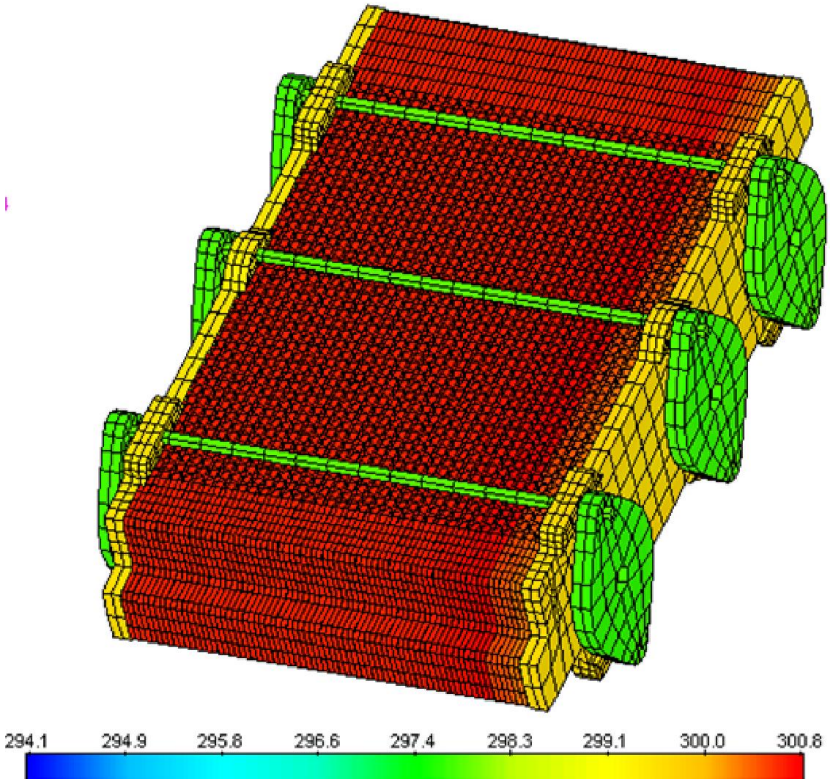

Figure 26: Heat flux for standalone FC stack for US06 cycle

Figure 27 illustrates a 2D thermal image obtained with the T620 Flir thermal camera illustrating the temperature profile across the FC stack at the beginning and end of the ADS tests. At the beginning of the test, the cells are colder as shown in (a) image. Towards the end of the test, cells much hotter as seen from (b). This is due to the fact the ADS draws maximum load current at an instant and sustains them for almost the entire period of 12 minutes. As given in Table 1, the cells at the inner region (temperature sensing 1) showed slightly higher temperature compared to that at the outer region (temperature at position 2) of the FC stack. Conjointly, Figure 28 exhibits the FC stack heat distribution and surface temperatures at various durations (0, 4, 8 and 12 minutes) under the FUDS driving test schedule. Even though the FUDS test lasted for 22 minutes, for our convenience the entire boundary conditions were shrunk to simulate for 12

minutes using the 3D thermal model. Such interpretation of the heat distribution helps understanding the thermal loads on the FC stack under implicit conditions, which can be used to assist the fabricator to establish a potent FC stack Thermal Management. Furthermore, it enables us to recuperate the stack packaging composition and identify packaging limitation at an early stage of design process. It is also noted that the temperature gradient of the stack is towards the center as already discussed in earlier chapters.

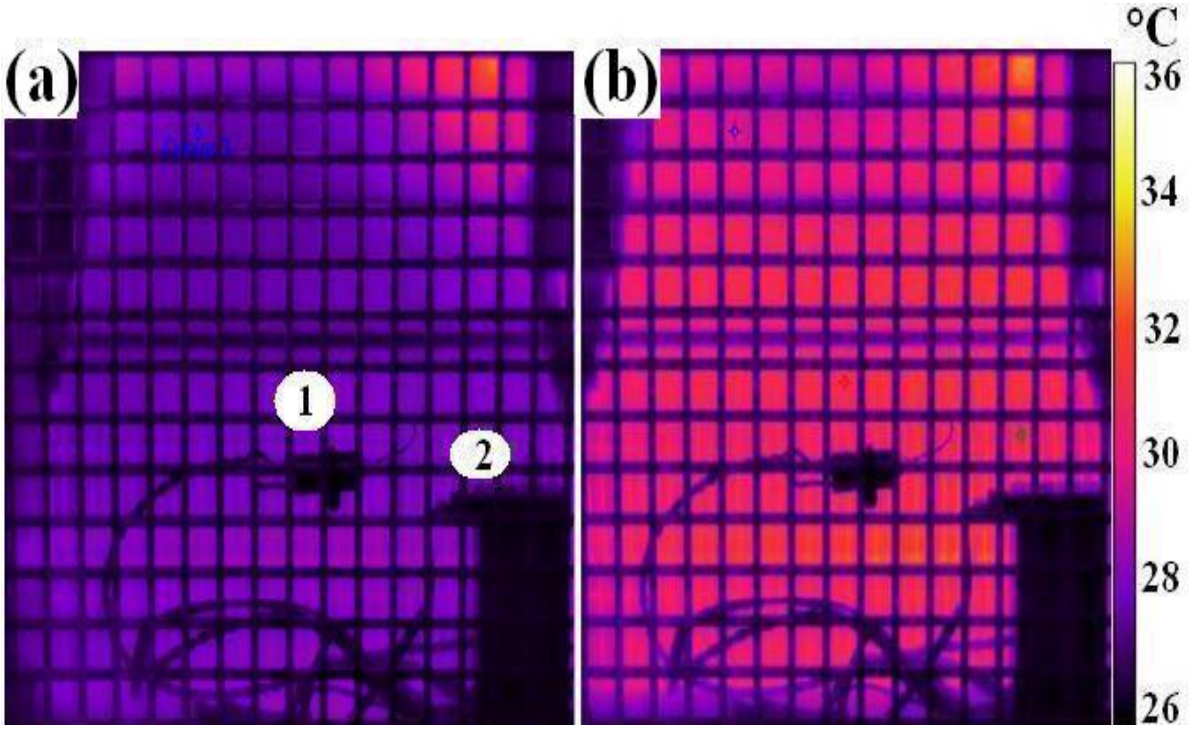

Figure 27: 2D thermal images showing temperature profile across the PEMFC stack (a) at the beginning and (b) at the end of 12 min.

Statistic	Image	Temperature sensing 1	Temperature sensing 2
Mean Temperature (start of test)	26.68	27.66	27.67
Mean Temperature (end of test)	27.34	31.21	30.53

Table 3: Temperature values across the thermal images

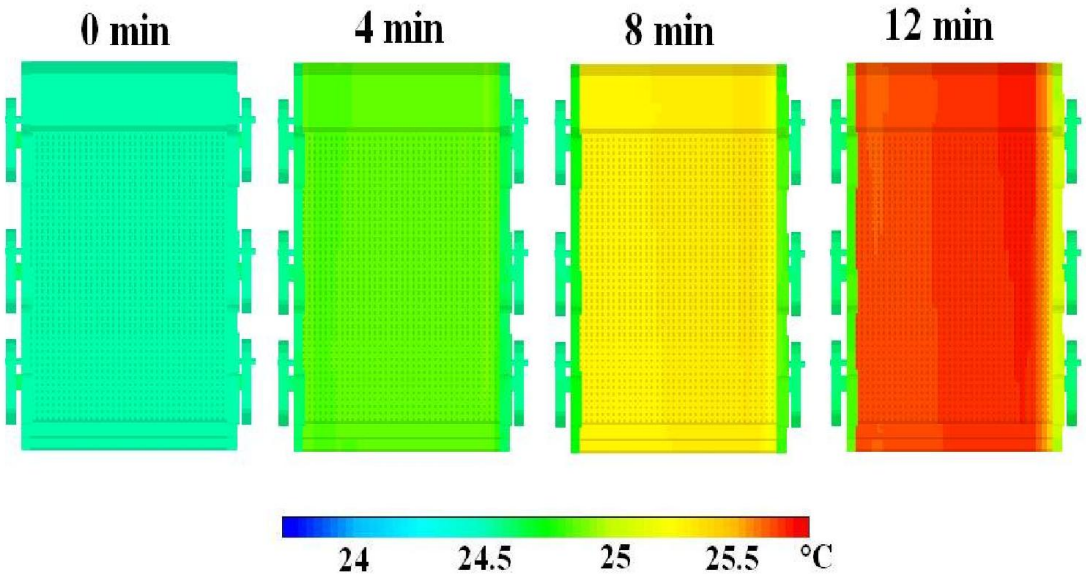

Figure 28: Heat distributions and surface temperature for the PEMFC stack under the FUDS driving test schedule for various duration.

Comprehending the transient thermal performance of the cells enables us to devise the cooling technique to control the operating temperature. This is primarily to prevent the FC from overheating, thereby maintain the overall operation and accuracy of the stack. To round up the physics of the cell and characterize the net heat rates by three modes i.e. conduction, convection & radiation, two positions are selected on the stack. These two positions include one at the center and other towards the edge from one side as illustrated in figure 29 highlighted with blue color.

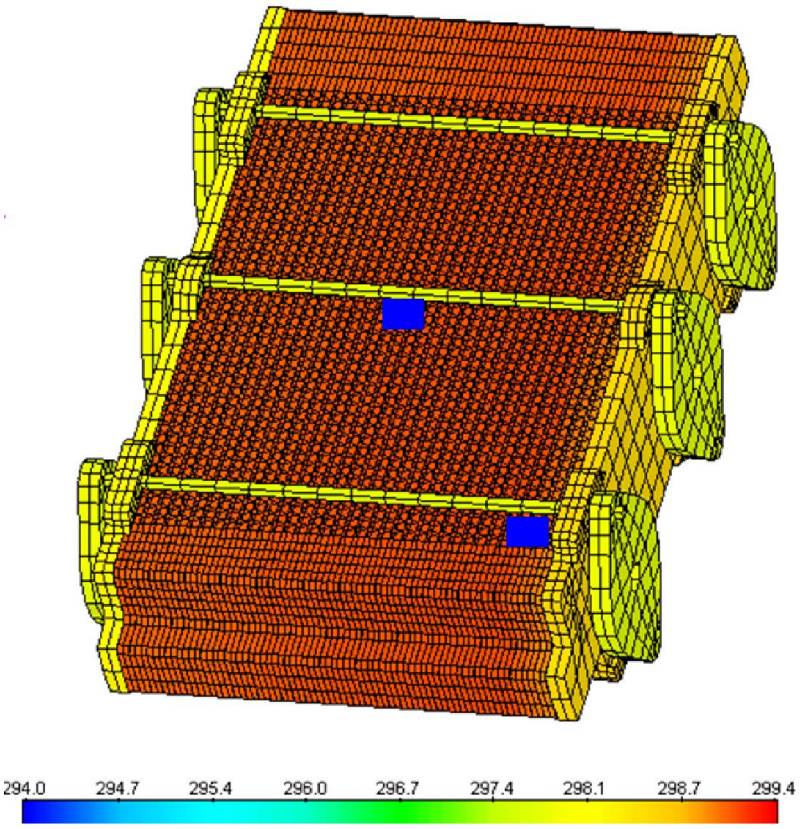

Figure 29: Pre-selected cell location

Both the surface temperature obtained from thermocouples and thermal model was plotted in contrast with actual temperatures recorded by the infrared detector of the complete stack as shown in figure 30 and figure 31 for ADS and FUDS test respectively. The main purpose of specific drive scheme (FUDS and ADS) under study was because these tow driving schedules show critical current flows on the FC stack. This shows that the FUDS replicated thermal characteristics of the cells under the transitory current fluctuations. On the other hand, the ADS represent very high steady state current flows of the stack cells. As detailed in figure 31, the model anticipated an exponential increase in the typical cells surface temperature of around 1^0C from the initial start temperature, in contrast to an increase of about 2^0C recorded by the IR thermal camera , under the FUDS drive cycle test which lasted for around 22 minutes. In the case of ADS test, the model

predicted an increase of surface temperature for the stack cells of about 2.2 ^{0}C in contrast to an increase of about 3.7 ^{0}C as noted by IR detector which lasted around for around 3 minutes depicted in figure 30. One important point to be noted is the variations in temperature in the profile by the model and actual surface temperature as measured by the thermocouples and the IR camera. These variations could be caused by three important factors:

- The typical surface temperatures as predicted by the IR camera were for the complete Fuel cell including the wires, interconnectors, insulations etc.
- Secondly, the model deals the FC stack as an assembly, even though the stack is a collection of 36 cells. Thus the model is equipped to extract the thermal attributes of each individual cells rather than the model as an entire assembly and plot the mean temperature of each cell. The same analogy was used for the two preselected cells which were taken into account to be compared with the surface temperature provided by the IR camera.
- The heat transfer by convection for the centre cell is low as compared to the cell towards the edge. The chances to remove heat by conduction and radiation are much less due less room to dissipate and heat transfer is done only through neighboring cells which can be seen in the temperature measurements by the

thermocouples.

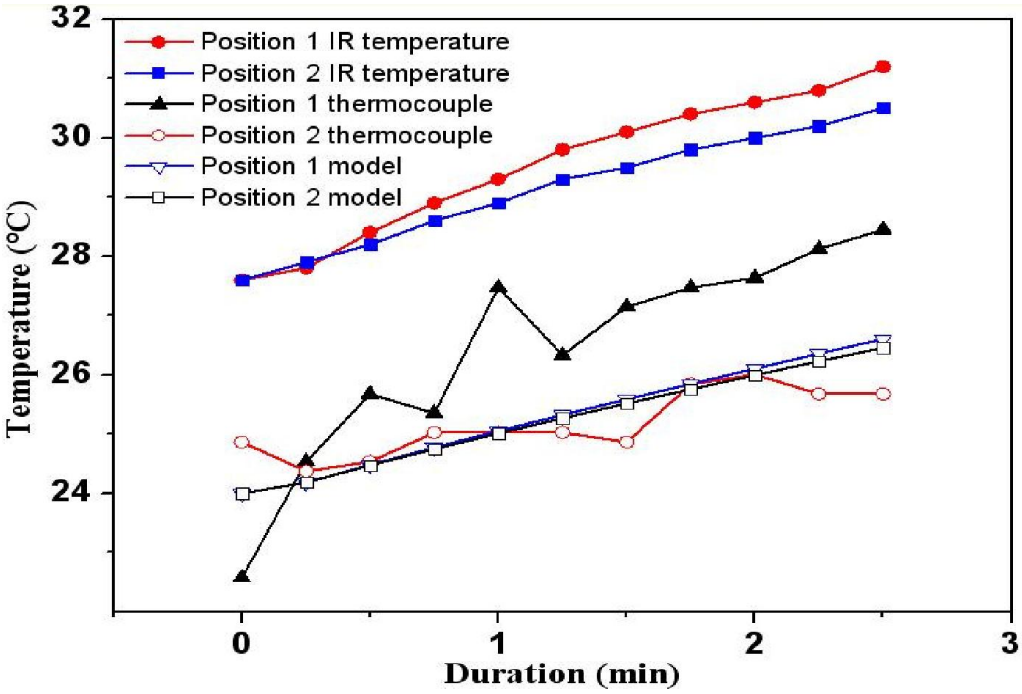

Figure 30: Surface Temperatures for the pre-selected battery cells for ADS test

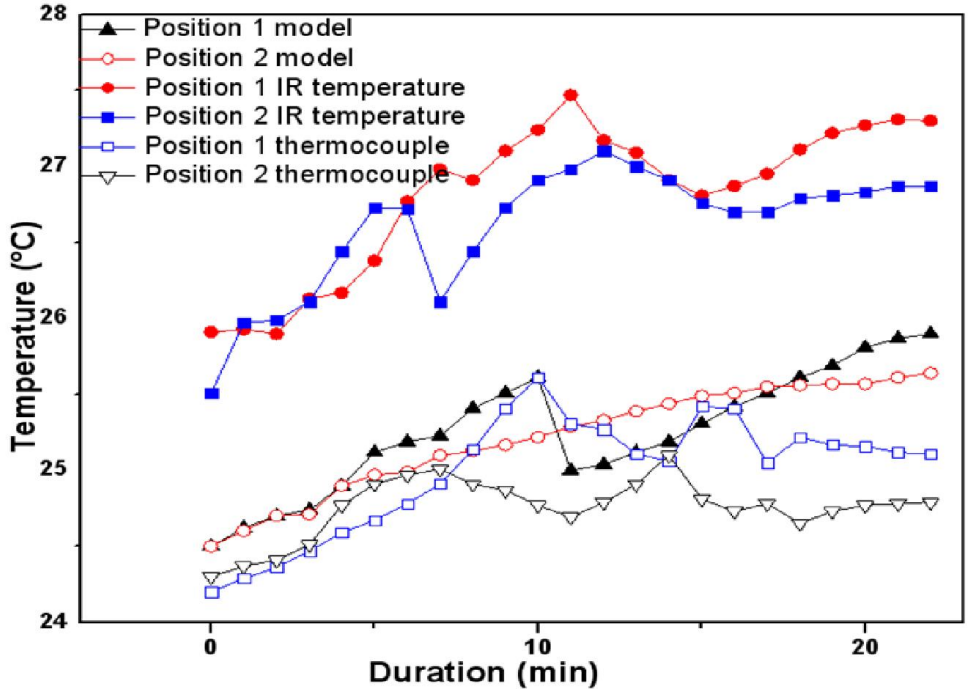

Figure 31: Surface Temperatures for the pre-selected battery cells for FUDS test

Similarly, the Net Heat exchange Rates (NHR) between two cells were evaluated to know about thermal action of various cells at different locations on the stack. This was done for the two pre-selected cells on the FC stack as displayed in Figures 32a and 32b. The figure illustrates the conductive, convective and radiative heat exchange rates for the pre-selected positions on the FC stack. This was performed to study the effect of packing and cooling strategies on the thermal attributed of the cells under transitory and steady state loading conditions. As the figure illustrates, the pre-selected location at the center has the outgoing net heat rate of about (0.006 W) approximately by convection and incident heat rate by conduction an average of (0.001W) approximately. While the radiation heat transfer rate to the surrounding environment was around 0 W through the test process. The net heat rate exchange between the two cell positions in the radiation mode, the cell at the corner and at the middle is almost same, wavering around 0 to 0.001 W. Usually, the heat exchange rate through radiation is lesser than compared to the one at the corner, but in this case there is connective heat transfer acting through surface of the stack. This is due the cooling fan behind, which actually draws the atmospheric air required to carry out the chemical process. The important aspect to note is that the pre-selected cells show variable NHR during the first 12 minutes of the artificial driving cycle and after 12 minutes it showed a steady NHR for rest of the ADS test.

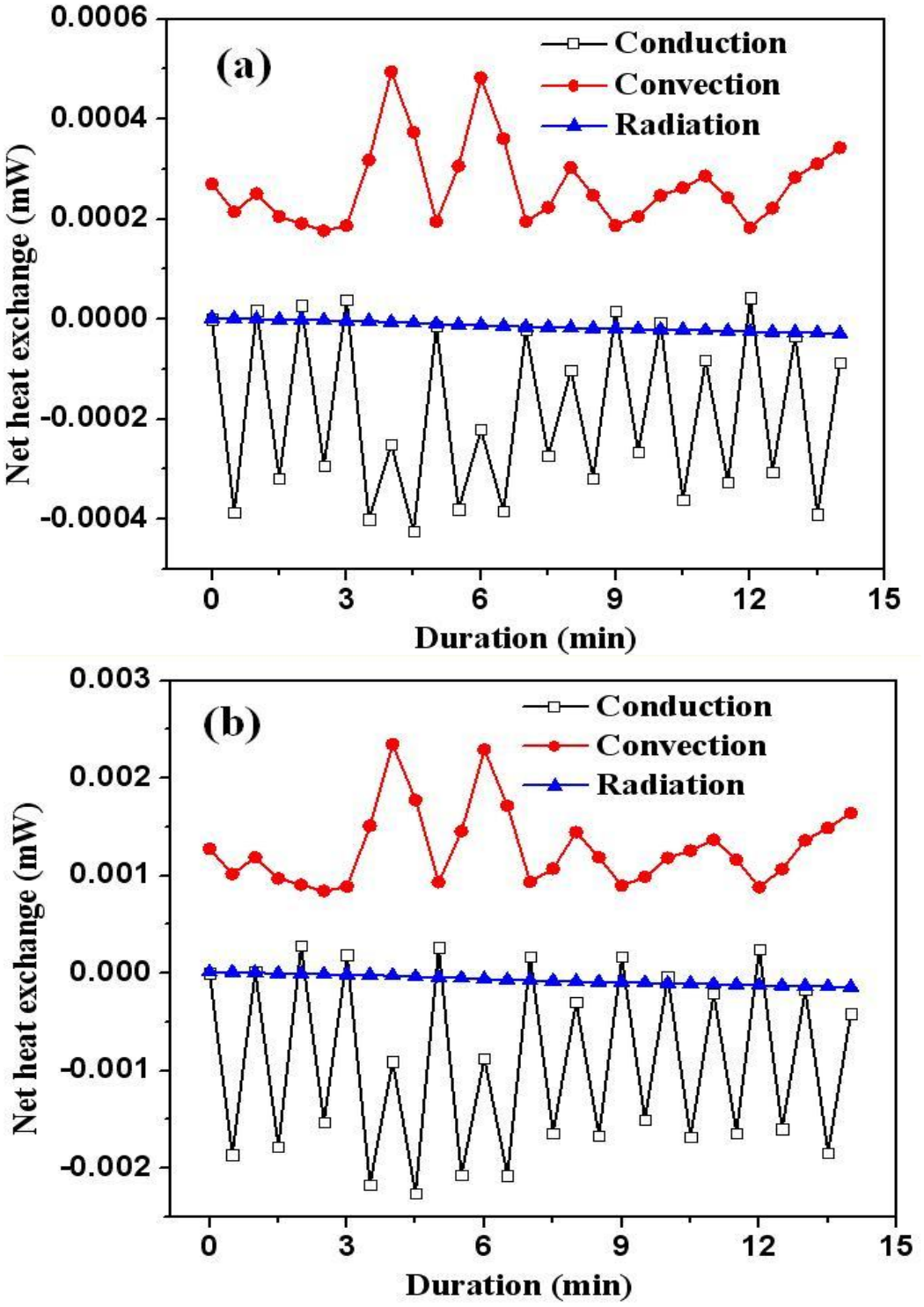

Figure 32: Net heat exchange rate by conduction, convection and radiation by temperature sensing at positions (a) 1 and (b) 2

The results obtained above can be used to contrive new thermal control scheme for employing new cooling pattern for perfect operation of stack under different various

patterns and environmental conditions. As a consequence, this model created a virtual environment which helps the design engineers to modify the design earlier in the development proceeds with less time, cost and effort. Furthermore, the Fuel cell is a proficient model in predicting the net heat exchange rates for geometrical parts and replicating the heat transmission into/out of the different modules.

5.3 FC performance characteristics

The drive cycle tests were conducted in order to obtain the thermal performance under controlled conditions such as load, temperature, current and voltage. In addition, the tests help arriving at the decisive boundary conditions for the FD duplication of the fuel cell model. The FC system is known to display thermal signature when it is operated under load. The results retrieved include: voltage, current, flow rates of hydrogen and air and actual surface temperature of the fuel cell as recorded by IR camera and the thermocouple as well. As already discussed, the flow rates of the Hydrogen and air depends on the load current and power drawn. Figure 33 manifests the results encountered during the FUDS drive cycle, depicting that the fuel cell performance parameters (voltage, current and temperature) change significantly. It has been noticed that the surface temperature of the fuel cell increases from 27.6 to 28.4 ^{0}C during the FUDS test.

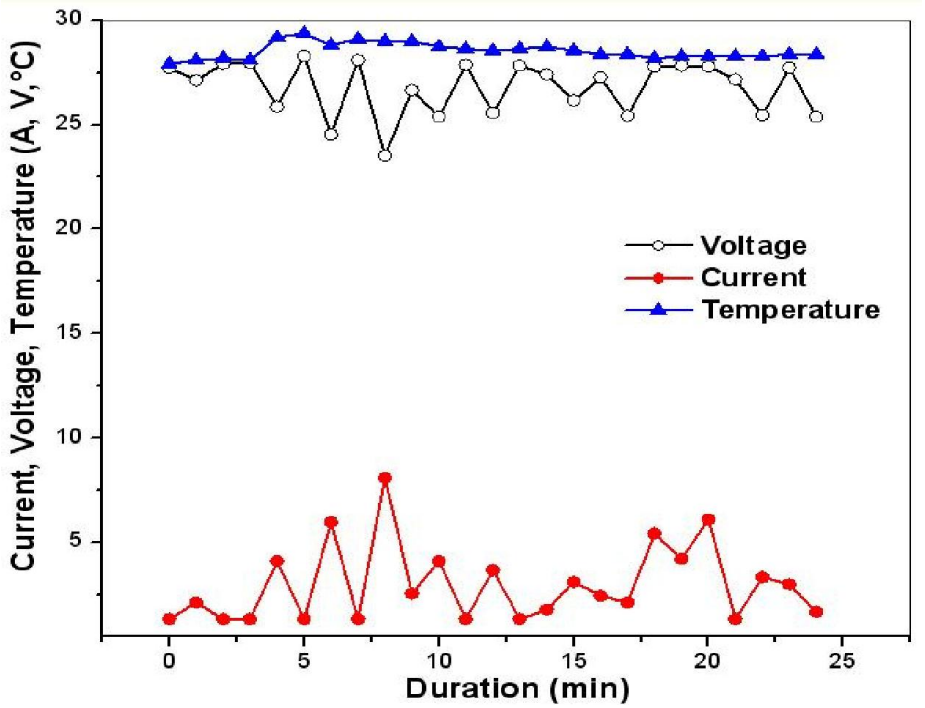

Figure 33: PEMFC stack temperature and performance characteristics under FUDS test.

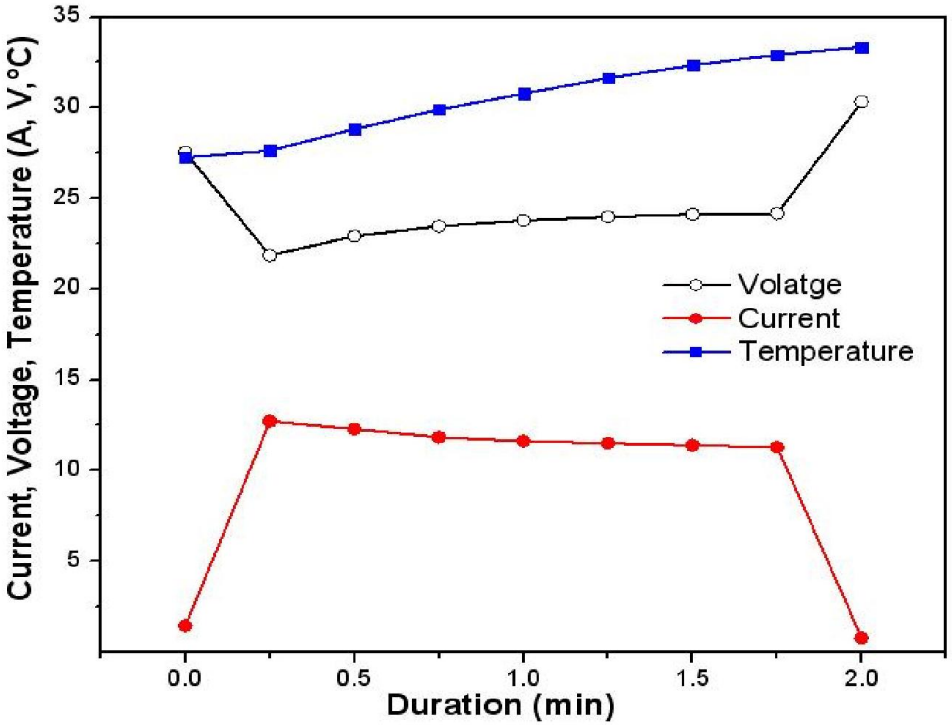

Figure 34: PEMFC stack temperature and performance characteristics under ADS test.

Additionally, the acceleration driving schedule validates the steady state performance of the fuel cell system at peak power demands as illustrated in Figure 34. The test results represent the surface temperature and the current flow at different vehicle speed intervals. It is to be noted that the fuel cell experience a steep increase in the current drawn.

5.4 Thermoelectric cooler

This model is tested for the ADS, as this drive cycle manifests greater thermal signature. It is noted that the temperature on the surface of the stack is lowered after the application of the thermo-electric cooler [39]. Furthermore, the temperature of the incoming air is not reduced too much, as it affects the performance of the fuel cell. The TE model is tested for the ADS driving test, as this shows the maximum thermal signature. Figure 35 demonstrates the application of thermoelectric modules to the model. The TE model is enforced in the differencing code simulator, the united effects of input heat to the hot side like the air flow and temperature, the output flow from the cold source, and the effective heat exchange competency of the sources can be comprehended in the single solver (RadTherm). There is a convective heat transfer due to the presence of the cooling fan behind the FC stack. This typically acts as a suction which pulls the atmospheric air through the thermoelectric modules which cools down the incoming air before hitting the stack cells.

As the power is drawn from the FC system, the heat flux across the stack increases. The incoming air passes through the aluminum fins in the duct. The fin is the cold junction of the TE module. The air is cooled by removing the heat and passed to the hot junction of the TE module, which is dissipated from the hot side. It is important that the air is not cooled too much; as it directly affects the performance of the FC system. The main

advantage of using a TE module is that, the above principle can be reversed such that the incoming air can be also heated up especially for cold start-up. The TE module can be optimized and interfaced with the control system of the FC. This enables for efficient cooling based on load requirements.

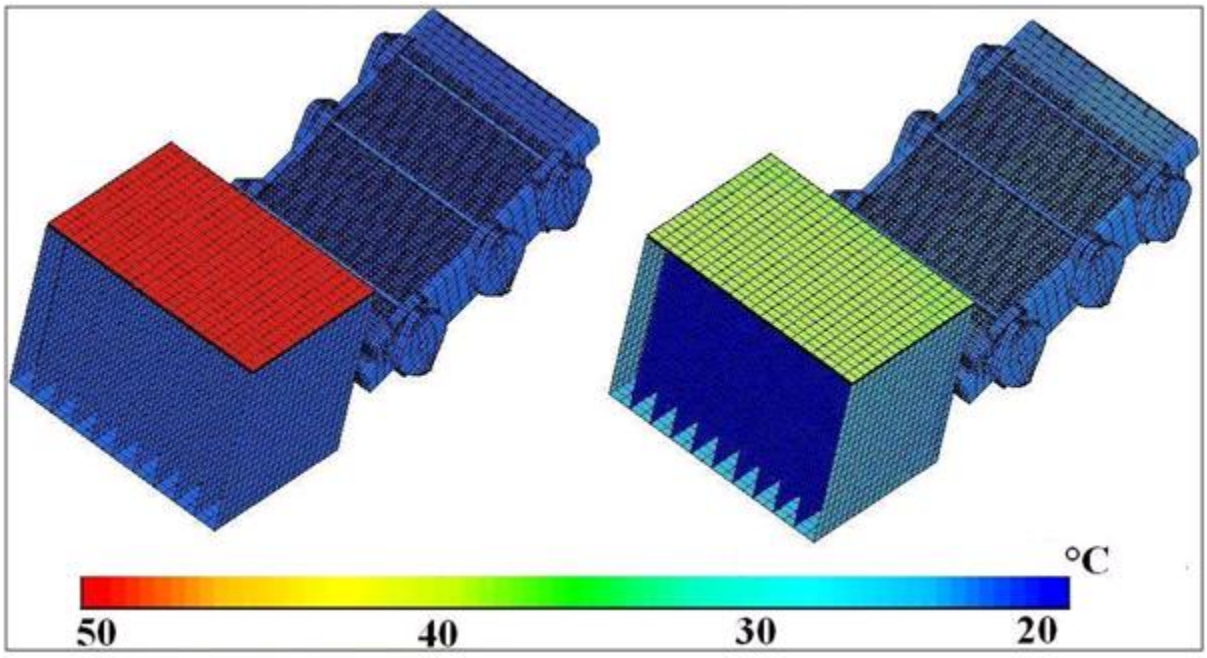

Figure 35: Thermoelectric module showing (a) with fins (b) Heat flux at the end of the ADS driving test as anticipated by the model

Figure 36 shows the average surface temperature across the FC stack with and without the TE modules, respectively. As the graph shows, the TE module enables to control the temperature across the stack within the operating range, such that the performance is unaffected. At around 2 minutes of operation, there is a sharp rise in current as per ADS driving test. The temperature of the incoming air on the cold side is reduced by heat removal. This maintains the temperature across the surface of the stack according to current drawn the stack, illustrating the control strategy instilled with the TE module.

The starting hot side is at 50 ^{0}C for ambient temperature of 23 ^{0}C is maintained. As the power drawn from the stack increases, the heat from inlet air passes to hot side from the cold side. The amount of heat load needed to remove and the desired cold-side temperature, enables to determine input voltage. The interfaced module is capable of producing 10 ^{0}C temperature difference (ΔT) when induced with open circuit voltage of 3.3 V. It is also noted that the temperature on the cold side is decreased by around 3-4 ^{0}C, this may be due to fact that there is a reduction in temperature on the hot-side [40].

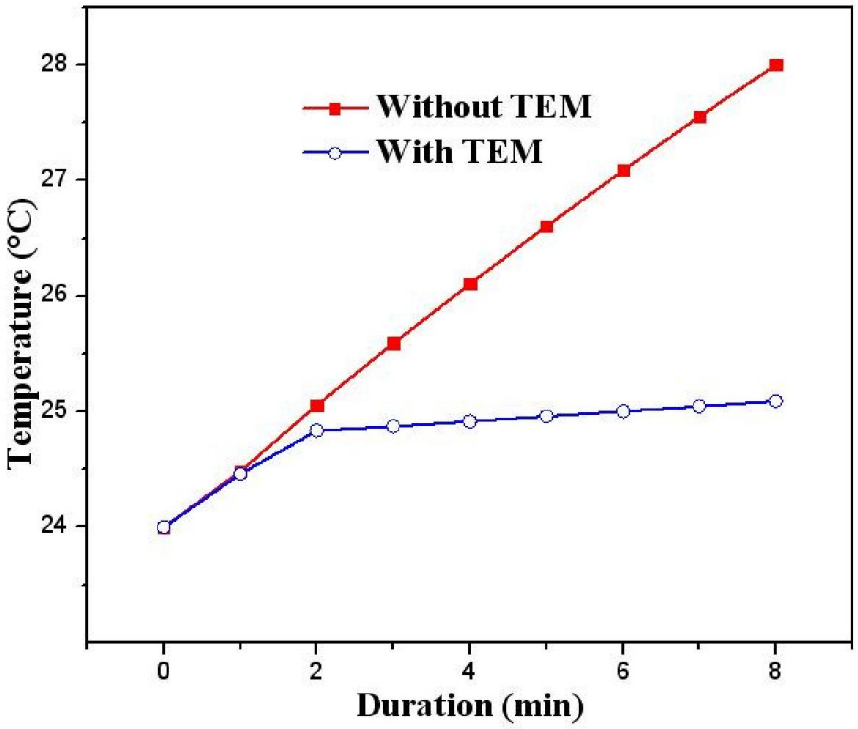

Figure 36: Surface temperature curves of the model with and without thermoelectric module.

CHAPTER SIX

6. CONCLUSION

6.1 Conclusions

The proposed work examined the augmentation of a comprehensive 3D thermal model for a PEM FC stack. An effective cooling strategy for automotive power trains with FC model was proposed, the temperatures was measured using thermocouples and thermal camera formed the base for thermal modeling. This involved distinctive procedure of extracting the boundary conditions, where a real time spatial and transient temperatures using the thermal camera. This procedure was performed during the standard driving cycles such FUDS, FHDS, etc., in excess to the custom made artificial cycle.

The entire Model was forged and justified for system running in HiL under these different standard and custom driving schedules. The 3D thermal model is refined using a FDC integrated with experimentally extracted boundary conditions including electric current, power, flow rates and temperature curves. The spatial and temporal temperature profiles of the proposed model reconcile with that of the experimental data of the FC stack as provided by the control unit of the FC. The solutions obtained show that the model is capable of predicting the thermal behavior of the fuel cell under controlled scheme (load, power, temperature and environmental conditions).

The FC stack were controlled in way that the current flows could be controlled in such a way that a realistic boundary conditions could be studied for net heat exchange rates by conduction, convection and radiation for all drive patterns which enables to analyze the thermal loads on the packs. Furthermore, the model can be used to validate the thermal performance for any corrections for vehicle power train including: material replacement,

rerouting and thermal packaging, validating any other different cooling strategies, and/or other design modifications may be applied to the system.

To extension for the cooling strategy, a scheme of simulation and optimization for a TE module has been contemplated based on the proposed modeling. The TE model of the inlet duct has been manifested and braced with the TE system model in FDC as a whole.

6.2 Improvements

This work enables us to develop extensive 3D simulation means for better thermal management for FC or hybrid powertrains. Almost all previous works concentrated on models which did not account for radiation heat transfer, which is the most important heat transfer mode in the power train system. In the addition to this, the thickness of the some larger components was actually ignored to trim the number of surfaces and make easier for the mesh generation process. A powerful meshing tool (ANSA) was used to construct a complete finite element model was generated to incorporate the parts with thermal conduction.

A more realistic approach was used here as inclusive boundary conditions retrieved from the stand alone FC under different loading conditions with a varied range of driving patterns were implemented. This enabled us to evaluate the complete thermal performance of the power train module under various loading schemes.

Application of the thermography technique using the IR FLIR camera focal array with very high resolution automated emissivity allowed us to validate the FC stack with non contact 2D spatial temperature measurement. This formed a primary verification of results obtained experimentally which could enabled the designer in lower down the

design time and cut the cost down. Ultimately this could reduce the necessity for crating expensive prototypes. Future research will focus on the effects on entire FC system to achieve optimized system modeling strategy.

REFERENCES

[1] Kandlikar S.G., & Lu Z., (2009). Fundamental Research Needs in Combined Water and Thermal Management within a Proton Exchange Membrane fuel cell stack under normal and cold-start conditions. J. Fuel Cell Science Technology, 6, 044001-13.

[2] Popovic, J., & Ferreira, J., (2005). An approach to Deal with Packaging in Power Electronics," Power Electronics- IEEE Transactions, 20(3), 550-557.

[3] Shahsavari. S (2012). Thermal analysis of air-cooled PEM fuel cells. International Journal of Hydrogen Energy, 37, 18261-71.

[4] Shimpalee, S. & Dutta, S. (2000). Distribution in PEM fuel cells. Numerical Heat Transportation, 38, 111-28.

[5] Nguyen, T., White R (1993) A water and heat management model for proton exchange membrane fuel cells. Journal of Electrochemical society, 140, 2178–2186.

[6] Matian, M. (2010). Application of thermal imaging to validate a heat transfer model for polymer electrolyte fuel cells. International Journal of Hydrogen Energy, 35(22), 12308-16.

[7] Del Real, AJ. (2007). Development and experimental validation of a PEM fuel cell dynamic model. Journal of Power Sources, 173, 310-24.

[8] Kandlikar, SG., & Lu, Z (2009). Thermal management issues in a PEMFC stack – A brief review of current status. Applied Thermal Engineering, 29, 1276-80.

[9] Djilali, N. (2007). Computational modeling of polymer electrolyte membrane (PEM) fuel cells: Challenges and opportunities. Energy, 32, 269-80.

[10] Sharifi, SM. (2010). Modelling and simulation of the steady-state and dynamic behavior of a PEM fuel cell. Energy, 35, 1633-46.

[11] Zong, Y. (2006). Water and thermal management in a single PEM fuel cell with non-uniform stack temperature. Journal of Power Sources, 161, 143-59.

[12] Bao, C. (2006). Analysis of the water and thermal management in proton exchange membrane fuel cell systems. International Journal of Hydrogen Energy, 29, 1040–57.

[13] Cao, TF. (2013). Numerical investigation of the coupled water and thermal management in PEM fuel cell. Applied Energy, 112, 1115–25.

[14] Musio, F. (2011). PEMFC system simulation in MATLAB-Simulink environment. International Journal for Hydrogen Energy, 36, 8045-52.

[15] Mayyas, AR. (2011). Comprehensive thermal modeling of a power-split hybrid power train using battery cell model. Journal of Power Sources, 196, 6588–94.

[16] Nexa 1200 User´s Manual (2014), Heliocentris Energy Systems. [ONLINE] Available http://www.heliocentris.com/; 2009. [Last Accessed 2014]

[17] FLIR T620. Thermal Imaging Camera (2014). [ONLINE] Available: http://www.flir.com/; 2013. [Last Accessed 2014]

[18] Math Works. Inc. MATLAB\SIMULINK. [ONLINE]. Available: http://www.mathworks com/. [Last Accessed 2014]

[19] Goyal, G. (2014). "Model Based Automotive System Integration: Fuel Cell Vehicle Hardware-In-The-Loop," Dissertation, Arizona State University, Mesa.

[20] Environmental Protection Agency, USA. (2013) Available: “http://www.epa.gov/” “Testing and Measurement Emissions”. [Last Accessed 2014].

[21] Application series from Fluent (2003). Under Hood Thermal management. Fluent Inco. Available: www.Fluent.com. [Last Accessed 2014].

[22] Govindasamy, V.P.M., (2004), "Thermal Modeling and Imaging of As-built Automotive Parts," Dissertation, University of Tennessee, Knoxville.

[23] Johns, KR. (1995). A Methodology for Rapid Calculation of Computational Thermal Modes. SAE, 951012.

[24] Schwenn, T. (2008). A Discretization Primer and Modeling Discussion, RadTherm Training, ThermoAnalytics Inc.

[25] Mayyas, AR. (2010). Comprehensive Thermal Modelling of power split hybrid power-train and electronics. PhD dissertation, Clemson University.

[26] Johnson, K. (1998). MuSES: A new heat and signature management design tool for virtual prototyping, Proceedings of Ninth Annual Ground Target Modeling and Validation Conference, Houghton, Michigan.

[27] Curran, A. R. (1995). Automated radiation modeling for vehicle thermal management. SAE International Congress & Exposition, Under hood Thermal Management Session, 950615.

[28] Mayyas, AR. (2011). Comprehensive thermal modeling of a power-split hybrid power train using battery cell model. Journal of Power Sources, 196, 6588–94.

[29] Valisetty, RR. (2004). Parallel MuSES for Infrared Signature Modeling of US Army Vehicles and Targets, Army Research Laboratory ARL-TR-328.

[30] Van den Oosterkamp, PF. (2006). Critical issues in heat transfer for fuel cell systems; Energy conversation management, 47, 3552-3561.

[31] Korukcu M. Ö., & Kilic, M., (2009). The usage of IR Thermography for the Temperature Measurements inside an Automobile Cabin. International Communications in Heat and Mass Transfer, 36(8), 872-877.

[32] Eads, L. (2000).Thermography. ASHRAE Journal, 42(3), 51-55.

[33] Astarita, T. (2006). Infrared thermography: an optical method in heat transfer and fluid flow visualization, Optics and Lasers in Engineering, 44, 261–281.

[34] Chevrette, P. (1986). Calibration of Thermal Imagers, Proceedings of the SPIE. The International Society for Optical Engineering, 661, 372-382.

[35] Smith, JA. (1999). Effect of Spatial Resolution on Thermal and Near-Infrared Sensing of Canopies," Optical Engineering, 38, 1413.

[36] Rowe DM, (1995). CRC Handbook of Thermo electrics, CRC Press.

[37] Chakib, A. (2011). Peltier Thermoelectric Modules Modeling and Evaluation. International Journal of Engineering, 5(1).

[38] Zhang, R. (2012). Optimized Thermoelectric Module-Heat Sink Assemblies for Precision Temperature Control. Journal of Electronic Packaging. 134(2), 021007.

[39] Camargo, JR. (2011). Principles of Direct Thermoelectric Conversion, InTech Europem.

[40] Chen, M. (2010). System modeling and validation of a thermoelectric fluidic power source: Proton Exchange Membrane fuel cell and Thermoelectric Generator (PEMFC-TEG). Journal of Electronic Materials, 39, 1593-1600.

APPENDIX

A: FLOW RATE & MODEL PARAMETERS

This section discusses the flow rate and the model parameters on the FDC solver. Based on the current drawn, flow rates of hydrogen and air, of the anode and cathode are calculated respectively. Generally, in a FC stack supplied with pure hydrogen, the fuel consumption can be obtained by,

$$\mathbf{m_{H2} = (1.05\times10^{-8})\ (P_S/V_{FC})} \quad \text{.....} \quad (1)$$

Where $m_{H2,}$ is the hydrogen mass flow rate (kg/s); $\mathbf{V_{FC}}$ is the FC voltage (V) and $\mathbf{P_S}$ is the stack electrical power (W), obtained from,

$$\mathbf{P_S = n.\ V_{FC}.\ i_{FC}} \quad \text{.....} \quad (2)$$

Where **n** is the number of cells used on the stack.

The air mass flow rate (kg/s) can be obtained using the equation in 3,

$$\mathbf{m_{air} = (3.57\times10^{-7})\ \lambda(P_S/V_{FC})} \quad \text{.....} \quad (3)$$

where, $\boldsymbol{\lambda}$ is the stoichiometric rate.